ISSN 1674-1056
http://cpb.iphy.ac.cn
http://iopscience.iop.org/cpb
中国物理 B
Chinese Physics
中国物理 Chinese Physics B

High-magnetic-field induced charge order in high-T_c cuprate superconductors

L X Zheng(郑立玄), J Li(李建), T Wu(吴涛)
Citation: Chin. Phys. B . 2019, 28(11): 117402 . **doi:** 10.1088/1674-1056/ab4575
Journal homepage: http://cpb.iphy.ac.cn; http://iopscience.iop.org/cpb

What follows is a list of articles you may be interested in

Nuclear magnetic resonance measurement station in SECUF using hybrid superconducting magnets

Zheng Li(李政), Guo-qing Zheng(郑国庆)
Chin. Phys. B . 2018, 27(7): 077404 . **doi:** 10.1088/1674-1056/27/7/077404

Structural phase transition, precursory electronic anomaly, and strong-coupling superconductivity in quasi-skutterudite $(Sr_{1-x}Ca_x)_3Ir_4Sn_{13}$ and $Ca_3Rh_4Sn_{13}$

Jun Luo(罗军), Jie Yang(杨杰), S Maeda, Zheng Li(李政), Guo-Qing Zheng(郑国庆)
Chin. Phys. B . 2018, 27(7): 077401 . **doi:** 10.1088/1674-1056/27/7/077401

Multiband nodeless superconductivity near the charge-density-wave quantum critical point in $ZrTe_{3-x}Se_x$

Shan Cui(崔珊), Lan-Po He(何兰坡), Xiao-Chen Hong(洪晓晨), Xiang-De Zhu(朱相德), Cedomir Petrovic, Shi-Yan Li(李世燕)
Chin. Phys. B . 2016, 25(7): 077403 . **doi:** 10.1088/1674-1056/25/7/077403

Hybrid crystals of cuprates and iron-based superconductors

Xia Dai(代霞), Cong-Cong Le(勒聪聪), Xian-Xin Wu(吴贤新), Jiang-Ping Hu(胡江平)
Chin. Phys. B . 2016, 25(7): 077402 . **doi:** 10.1088/1674-1056/25/7/077402

Spin, charge, and orbital orderings in iron-based superconductors

Jiang Qing, Kang Yao-Tai, Yao Dao-Xin
Chin. Phys. B . 2013, 22(8): 087402 . **doi:** 10.1088/1674-1056/22/8/087402

TOPICAL REVIEW — Fundamental research under high magnetic field

High-magnetic-field induced charge order in high-T_c cuprate superconductors*

L X Zheng(郑立玄)[1], J Li(李建)[1], and T Wu(吴涛)[1,2,3,4,5,†]

[1] Hefei National Laboratory for Physical Science at Microscale, University of Science and Technology of China, Hefei 230026, China
[2] Key Laboratory of Strongly-coupled Quantum Matter Physics, University of Science and Technology of China, Chinese Academy of Sciences, Hefei 230026, China
[3] CAS Center for Excellence in Superconducting Electronics (CENSE), Shanghai 200050, China
[4] CAS Center for Excellence in Quantum Information and Quantum Physics, Hefei 230026, China
[5] Collaborative Innovation Center of Advanced Microstructures, Nanjing University, Nanjing 210093, China

(Received 26 July 2019; revised manuscript received 12 September 2019; published online 1 November 2019)

In the last few years, charge order and its entanglement with superconductivity are under hot debate in high-T_c community due to the new progress on charge order in high-T_c cuprate superconductors $YBa_2Cu_3O_{6+x}$. Here, we will briefly introduce the experimental status of this field and mainly focus on the experimental progress of high-field nuclear magnetic resonance (NMR) study on charge order in $YBa_2Cu_3O_{6+x}$. The pioneering high-field NMR work in $YBa_2Cu_3O_{6+x}$ sets a new stage for studying charge order which has become a ubiquitous phenomenon in high-T_c cuprate superconductors.

Keywords: charge order, cuprates, nuclear magnetic resonance, $YBa_2Cu_3O_{6+x}$ superconductors, competing order

PACS: 76.60.–k, 74.25.nj, 74.72.–h, 71.45.Lr **DOI:** 10.1088/1674-1056/ab4575

1. The tale of stripe in high-T_c cuprates

After thirty years discovery of high-T_c cuprate superconductor, their physical mechanism is still in suspense. As we know, the parent materials of high-T_c cuprates are widely accepted as Mott insulator in which all the electrons are localized by on-site Coulomb interaction U. When holes are doped into the two-dimensional CuO_2 plane, the Mott insulating phase is converted into a superconducting phase with appropriate hole concentration.[1] However, besides superconducting order, the doped holes could have tendency to build up other symmetry-breaking state which competes with the d-wave superconducting order.[2–7] In fact, there is indeed a very complicated doping dependent phase diagram in high-T_c cuprates[8] as shown in Fig. 1. One thread to decode the high-T_c puzzle is whether the competition with a symmetry-breaking electronic state underlied high-T_c superconductivity plays a key role on the complexity of high-T_c cuprates. Several experiments are suggestive of electronic-liquid-crystal phases,[9–19] of which an extreme version is 'stripe order': Charge filaments are embedded in a background of ordered spins as shown in Fig. 2. The first direct evidence of stripe order in a cuprate dates back to the discovery of stripes in $La_{1.48}Nd_{0.4}Sr_{0.12}CuO_4$.[20] Later, the local evidence for the charge stripe order was found by scanning tunneling microscopy (STM) in Bi-based cuprates,[21] in which the atomically flat surface enabled the real space image of charge stripe order in this system.[21–23]

Although stripe order has been definitely confirmed in high-T_c cuprates,[20–23,25–33] whether it is an intrinsic phenomenon to all of high-T_c cuprates is under strong debate. One critical argument against stripe is that static stripe order was just found in doped La_2CuO_4 family which is very disorder.[1] Searching stripe order in other cleaner cuprate families is essential to clarify the role of stripe physics in high-T_c cuprates.

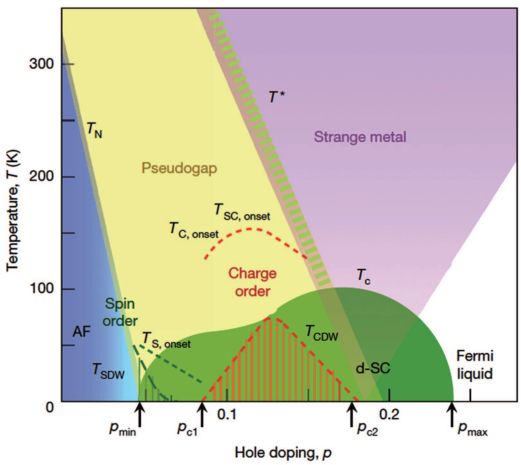


Fig. 1. Electronic phase diagram of high-T_c cuprates (from Ref. [8]).

In 2007, the observation of quantum oscillation in high-quality underdoped $YBa_2Cu_3O_{6+x}$ single crystal shed light on this issue.[34–36] This breakthrough suggests that, at least under high magnetic field, certain symmetry broken order

*Project partially supported by the National Natural Science Foundation of China (Grant Nos. 11522434 and U1532145), the Recruitment Program of Global Experts, China, and the Chinese Academy of Sciences Hundred Talent Program.

†Corresponding author. E-mail: wutao@ustc.edu.cn

© 2019 Chinese Physical Society and IOP Publishing Ltd

emerges to reconstruct the Fermi surface and produces closed Fermi pocket corresponding to quantum oscillation.[14–16] It shows great potential to search stripe order in such very clean and "90 K" cuprate family. A new legend on stripe is coming. In 2011, stimulated by quantum oscillation experiment, high-field ^{63}Cu nuclear magnetic resonance (NMR) experiment successfully found stripe order in the underdoped $YBa_2Cu_3O_{6+x}$.[37] It was found that while superconductivity is suppressed by external magnetic field, stripe order eventually emerges instead of superconducting order. In sharp contrast to stripe order observed in other cuprates, the stripe found in underdoped $YBa_2Cu_3O_{6+x}$ is purely charge stripe without following spin order. Benefit from the absence of spin order, this is the first time to successfully detect charge stripe by high-field NMR technique in cuprates. Moreover, due to oxygen ordering structure, the filled CuO chain was found to be able to pin the charge-rich part of charge stripe, which allows ^{63}Cu and ^{17}O NMR to distinguish one-dimensional (1D) charge stripe from other charge order patterns. In the following section, we would firstly explain how the NMR technique detects a charge modulation in a material.

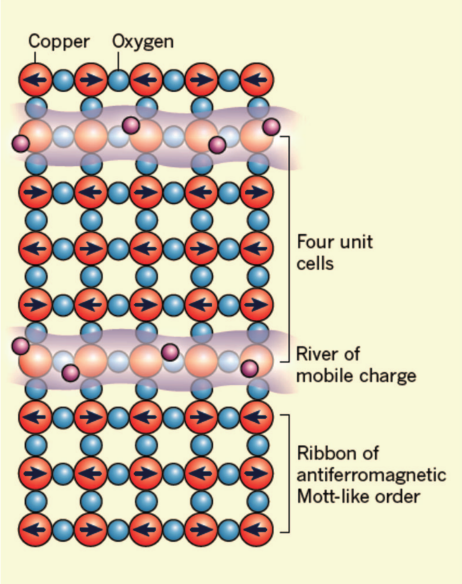


Fig. 2. Stripe-like electronic order in cuprates (from Ref. [24]).

2. How does NMR technique detect charge modulation in a material?

In condensed matter physics, charge density wave (CDW) or charge order (CO) is a spatial modulation of electronic charge density with specific periodicity and directions (q-dependent) either commensurate or incommensurate with background lattice. As a spontaneous symmetry broken state, it generates a super-lattice structure which locally modifies the charge environment deviating from a uniform distribution. Such modulations on electronic degree of freedom are also seen by nuclei through electron–nucleus hyperfine interactions. Both static and dynamical properties of such phases can be sensitively detected by solid state nuclear magnetic/quadrupole resonance (NMR/NQR) measurements.

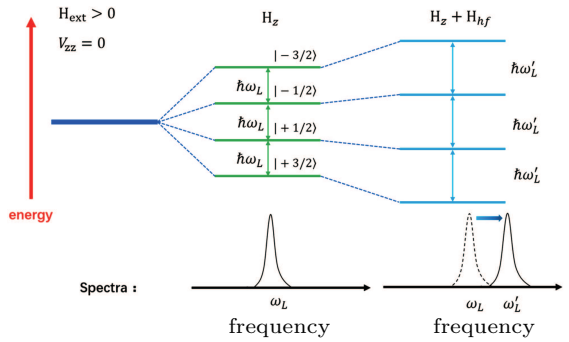


Fig. 3. Sketch of the energy level and the NMR spectra of nucleus with $I = 3/2$. The Knight Shift aroused by electron–nucleus hyperfine interaction is involved while without consideration of quadrupolar interactions.

In NMR spectroscopy measurements, the frequency shift, line broadening, or line splitting of the NMR/NQR spectra are key quantities to characterize CDW/CO. Unlike the conventional diffraction methods, as a sensitive local probe, NMR/NQR could be done with extremely high energy and position resolutions when using high-quality single crystals. In NMR spectroscopy, Knight shift (K) measures the percent shift of the resonance frequency from an isolated nucleus in an external magnetic field ($H_{\rm ext}$) with barely Zeeman splitting shown in Fig. 3 ($I = 3/2$ nuclei is taken as an example). Actually, Knight shift can be taken as an additional effective field experienced by the nuclei in crystals which is originated from the electron–nucleus hyperfine interaction. It contains detail information about the interaction. Generally, the magnetic hyperfine interaction between electron and nucleus is described as[38]

$$H_{\rm hf} = \gamma_{\rm n}\gamma_{\rm e}\hbar^2 \boldsymbol{I}\cdot\left[\left(3\frac{(\boldsymbol{S}\cdot\boldsymbol{r})\cdot\boldsymbol{r}}{r^5} - \frac{\boldsymbol{S}}{r^3}\right) + \frac{8\pi}{3}\boldsymbol{S}\delta(\boldsymbol{r}) + \frac{\boldsymbol{L}}{r^3}\right]. \quad (1)$$

The first term and second term describe the dipolar interactions between the nuclear spin and the electronic spin (with p-, d-, f-orbital characters) and the Fermi contact contributions (with s-orbital characters), respectively. The last term represents the orbital interaction between the nuclear spin $\boldsymbol{I}$ and the angular momentum $\boldsymbol{L}$ of the electron which usually contributes a temperature independent shift $K_{\rm orb}$ relative to Zeeman splitting. The first two terms contribute the spin part of the Knight shift $K_{\rm spin}$ which is usually temperature dependent and directly related to the electronic configurations near $E_{\rm F}$ and sensitively affected by even subtle reconstructions in the electronic structure. It can be rewritten as

$$K_{\rm spin} = A_{\rm s}\chi_{\rm s}/g_{\rm e}\mu_{\rm B}\gamma\hbar, \quad (2)$$

where $A_{\rm s}$ is the hyperfine coupling constant, and $\chi_{\rm s}$ is the uniform local spin susceptibility. In the CDW/CO state, the spatially modulated conduction electron density $\rho(r)$ will consequently produce a local modulation of $K_{\rm spin}(r)$ by changing

χ_s. Assuming a linear correlation between the CDW amplitude and the local resonance frequency ω_i at a nuclear site r_i, one obtains[39]

$$\omega_i = \omega_0 + \omega_1 \sum_j \cos(q_j \cdot r_i + \phi_j), \tag{3}$$

where $\omega_0 = \omega_{\rm ref}(1+K_0)$, K_0 is the Knight shift corresponding to uniform electron density. ω_1 is the modulation amplitude due to the conduction electron density of states which is assumed to be proportional to the CDW amplitude. q_j are the CDW wave vectors which can be commensurate or incommensurate with the lattice constants. ϕ_j are the CDW phases. This kind of NMR spectra analysis has been widely used to detect CDW states as shown in Fig. 4.

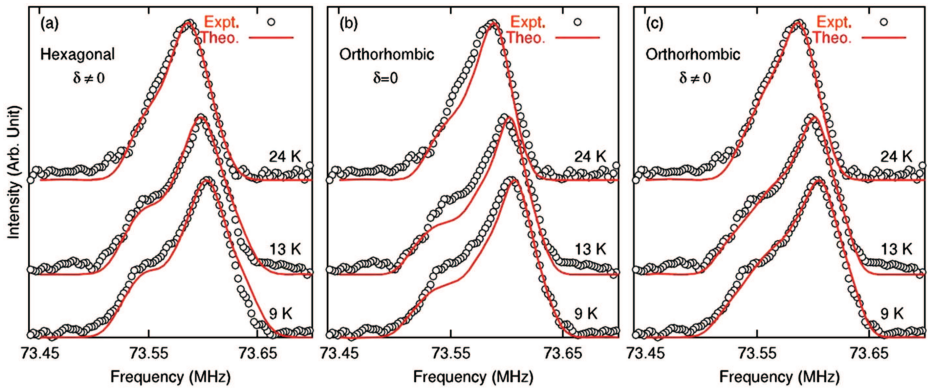


Fig. 4. The ^{93}Nb NMR spectra of $NbSe_3$ at 24 K, 13 K, and 9 K. The solid line represents the theoretical fitting, using the same equation with different physical cases (from Ref. [39]).

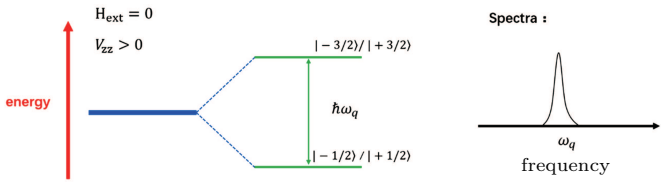


Fig. 5. Sketch of the energy level and the NQR spectra of nucleus with $I = 3/2$.

Besides the Knight shift modulated by CDW/CO, the quadrupole nuclei (nuclear spin $I > 1/2$) with non-cubic symmetrical environment ($V_{zz} \neq 0$) is often taken as a particular local probe of such state since it reveals the sign, magnitude, symmetry, and orientation of the electron field gradient tensor (EFG).[40] The quadrupolar Hamiltonian H_Q which describes the interactions between the quadrupole moment Q of the nucleus and the electric field gradient V is expressed as

$$H_Q = \frac{1}{6}\sum_{\alpha\beta} V_{\alpha\beta} Q_{\alpha\beta} = \frac{\hbar\omega_q}{2}\left[I_z^2 - \frac{I(I+1)}{3} + \frac{\eta}{6}(I_+^2 + I_-^2)\right], \tag{4}$$

where $\omega_q = \frac{3eQV_{zz}}{2I(2I-1)\hbar}$. V_{zz} can be chosen as the maximum component of diagonalized EFG elements along the principle axis ($|V_{zz}| \geqslant |V_{yy}| \geqslant |V_{xx}|$). η is the asymmetry parameter defined as $(V_{yy}| - |V_{xx}|)/V_{zz}$. For a nuclear spin $I = 3/2$ in zero magnetic field, the NQR frequency is

$$\omega_{\rm NQR} = \frac{3eQV_{zz}}{2I(2I-1)\hbar}\sqrt{1+\frac{\eta^2}{3}}. \tag{5}$$

With axial symmetry ($\eta = 0$), $\omega_{\rm NQR} = \omega_q$ as sketched in Fig. 5. Through implementation of NQR measurements, the magnitude or periodicity of electronic density modulation and the asymmetry properties may be elucidated. When the CDW/CO sets in, beyond the lattice EFG experienced by the nuclei (Fig. 6), the modulated electron density generating q-dependent spatially non-equivalent sites other than the structural sites is the key of these experiments.

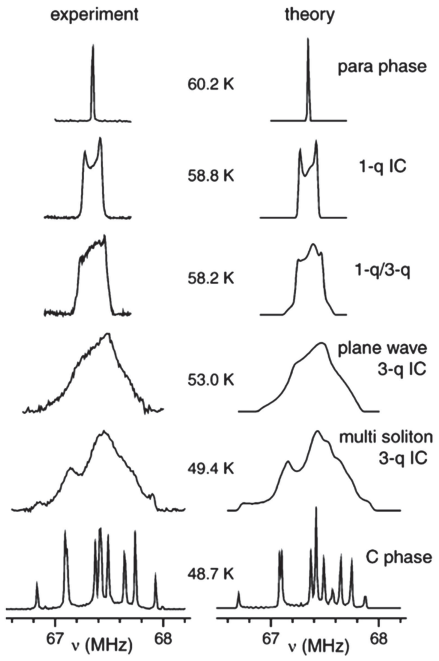


Fig. 6. Comparison between the observed and theoretical ^{75}As NQR lineshapes in proustite (from Ref. [41]).

One can also detect the quadrupolar shift of the NMR spectra to extract more comprehensive parameters on the electronic charge distribution in CDW/CO states as illustrated in Fig. 4. The total Hamiltonian H_t of quadrupolar nuclei in an arbitrary external magnetic field is

$$H_t = H_0 + H_Q$$

$$= \hbar\omega_L' I_z + \frac{\hbar\omega_q}{2}\left[I_z^2 - \frac{I(I+1)}{3} + \frac{\eta}{6}(I_+^2 + I_-^2)\right], \quad (6)$$

where $H_0 = H_z + H_{\rm hf}$, the intrinsic Knight shift is contained in ω_L', since the external magnetic field determines a specific direction for the nuclear spin system (I_z), the quadrupolar Hamiltonian will be angular dependent. With the definition of Euler angles, one can easily derive the angular dependent quadrupolar Hamiltonian which commutes with I_z[42]

$$H_Q(\theta,\phi) = \frac{\hbar\omega_Q}{6}\frac{3\cos^2\theta - 1}{2} + \frac{\eta}{2}\sin^2\theta\cos 2\phi\left(3I_z^2 - I(I+1)\right), \quad (7)$$

where θ is the polar angle of the external magnetic field in the principle axis of the EFG tensor, and ϕ is the azimuthal angle. Note that under the high magnetic field condition ($H_0 \gg H_Q$), H_Q can be taken as a perturbation, the first order correction will give the generation of satellite peaks. e.g., the case of $I = 3/2$ as shown in Fig. 7.

$$\omega_{m,m+1} - \omega_L' = \omega_Q\frac{3\cos^2\theta - 1}{2} + \frac{\eta}{2}\sin^2\theta\cos^2\phi\left(m + \frac{1}{2}\right). \quad (8)$$

Since the shift brought to the central-transition line only exists in higher order corrections, through detection of the shift or linewidth of the satellites and comparing it to the central-transition line, one can identify the quadrupolar contributions from the magnetic one. By measuring the angular dependent spectra of high quality single crystals, one can get the detail parameters of the CDW/CO phases such as the EFG tensors, the degree of homogeneity/inhomogeneity, the magnetic shift contributions, and so on.

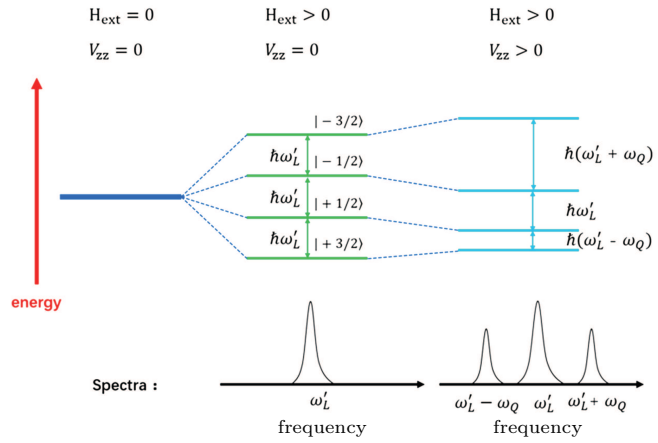


Fig. 7. Sketch of the energy level and the NMR spectra of nucleus with $I = 3/2$ with only consideration of quadrupolar interactions.

3. High-field NMR study on charge stripe order in YBCO

In this section, we will briefly review the high-field NMR progress on charge stripe in underdoped YBCO.

As we mentioned above, stimulated by quantum oscillation experiment in 2007, searching symmetry-breaking state under high magnetic field becomes an urgent task in high-T_c community. However, many important techniques are not available under high magnetic field, such as neutron scattering and angle resolved photoemission spectroscopy (ARPES). Therefore, NMR technique becomes a unique probe to detect symmetry-breaking state under high magnetic field. At the end of 2009, the Grenoble NMR group started the exploration on symmetry-breaking state in underdoped YBCO with ortho-II ordering structure at Grenoble high magnetic field lab. As shown in Fig. 8, the ortho-II ordering structure leads to two distinct planar Cu NMR sites: Cu2F are those Cu located below oxygen-filled chains and Cu2E those below oxygen-empty chains.[43] As shown in Fig. 9, these two distinct planar Cu sites could be easily resolved on quadrupole satellite of ^{63}Cu spectra. Such site-selective NMR gives us a possibility for spatial resolution of the following charge ordering state. The main finding in the first high magnetic field NMR experiment is shown in Fig. 9. The satellite for Cu2F site splits into two peaks below T_c under the high magnetic field along c-axis. At the same time, there is also a Knight shift splitting on the central line of Cu2F. Based on a detailed NMR analysis, both of quadrupole and Knight shift splittings are ascribed to the emergence of charge ordering state as we learned above. If we used the quadrupole splitting as an order parameter, its temperature dependent evolution looks like a second order phase transition. On the other hand, the above splittings on both Knight shift and quadrupole frequency are only found at Cu2F site but absent at Cu2E site as shown in Fig. 9.

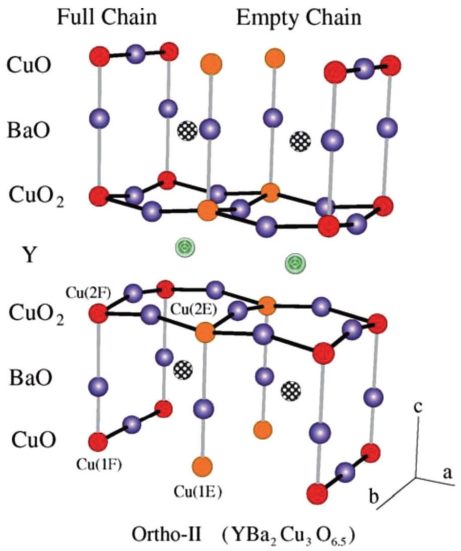


Fig. 8. The crystal structure of ortho-II YBCO (from Ref. [43]).

This result could be used to constrain the charge ordering pattern in space. As shown in Fig. 10, there are two kinds of possible charge ordering patterns that could fit the NMR results. However, the first one seems unphysical in real case. Then, the only plausible choice is the second one which is the same charge ordering pattern with a uniaxial 4a

period as the previous stripe order found in LNSCO.[20] But, in YBCO, there is no spin order coupled with charge order. This result has a strong implication on the quantum oscillation experiment, suggesting that the charge order reconstructs the Fermi surface and creates Fermi pockets in YBCO. Since the splitting due to charge ordering only happens at high magnetic field, it strongly suggests that the charge order is a field-induced phenomenon and would be hidden in the superconducting dome without applying any external field. Although such charge order only appears under high magnetic field, it is not simply induced by applying a magnetic field within CuO_2 plane as shown in Fig. 9. Because the upper critical field for the superconducting state is highly anisotropic in cuprates, the superconducting state is quite robust under magnetic field within CuO_2 plane.

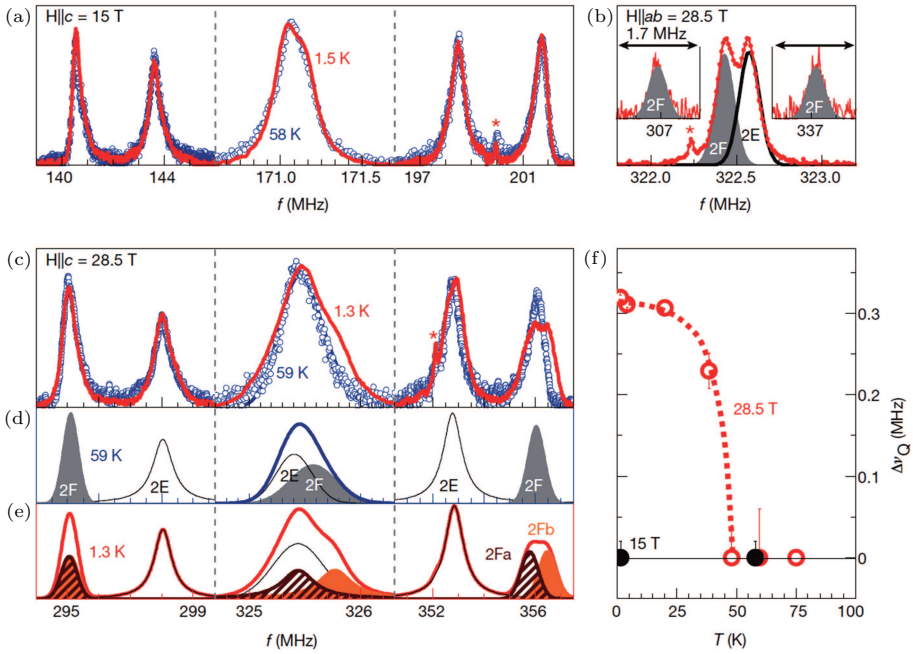


Fig. 9. High-field NMR spectra of $YBa_2Cu_3O_{6.54}$ (from Ref. [37]).

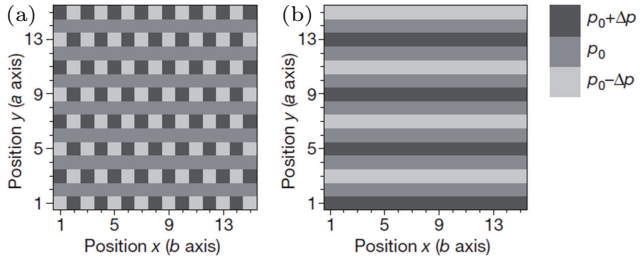


Fig. 10. Charge density modulations compatible with NMR spectra (from Ref. [37]).

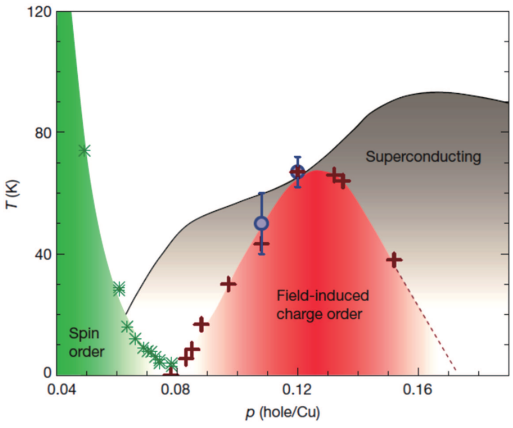


Fig. 11. Phase diagram of underdoped $YBa_2Cu_3O_y$ (from Ref. [37]).

Therefore, the field-induced charge order is actually caused by the suppression of superconducting state under the external magnetic field. It suggests that the charge order is a competing order of the superconducting state. A new phase diagram is proposed for YBCO as shown in Fig. 11, in which a field-induced charge order is peaked around 1/8 hole concentration and beneath the superconducting dome. This is a definite evidence for a long-range charge order in a clean cuprate superconductor family. It strongly suggests that charge order is an intrinsic phenomenon in high-T_c cuprates and it shows a strong correlation with the superconducting state.

Following the pioneering ^{63}Cu NMR experiment, the field-induced charge order was further verified by ^{17}O NMR experiment.[44] As shown in Fig. 12, charge order induced quadrupole splitting is also observed on the satellite of ^{17}O NMR spectra. Due to more remarkable splitting, the precise field-dependent order parameter of charge order could be extracted from the field dependent splitting of the ^{17}O NMR spectra. As shown in Fig. 13, the critical field of the field-induced charge ordering state shows a V-shape doping dependence corresponding to the doping dependent upper critical field of the superconducting state, which also suggests a close correlation between superconducting state and charge ordering

state. In a short summary, both ^{63}Cu and ^{17}O NMR spectra exhibit unambiguous and consistent evidence for a field-induced charge order in underdoped YBCO. Such field-induced charge order is a dominating competing order for superconductivity around 1/8 hole concentration and is hidden beneath the superconducting dome. When the superconducting state is killed by the external magnetic field, the competing charge order would appear through a second-order quantum phase transition, which is driven by the high magnetic field (Fig. 13).

Following the discovery of NMR works, a fluctuating CDW has also been found far above T_c in (Y, Nd)$Ba_2Cu_3O_{6+x}$ by resonant soft x-ray scattering even without applying external magnetic field.[45] Two resonant peaks corresponding to CDW signal were observed at (0.31, 0) and (0, 0.31) of the in-plane reciprocal space. They are different from the commensurate value of 1/3 so imply an incommensurate CDW. The temperature-dependent evolution of CDW signal in $YBa_2Cu_3O_{6.6}$ compound is shown in Fig. 14. The CDW signal starts to increase and becomes narrow upon cooling below 150 K until T_c. The correlation length of CDW can be roughly estimated by the reciprocal of the linewidth, which reaches the maximal value of 16a at T_c. The authors claimed that the above behavior of correlation length is more relative to a fluctuating CDW rather than a static CDW. Below T_c, a sudden suppression of intensity happens, which implies a competition between CDW and superconductivity. An interesting detail is that the intensities of the above two CDW signals are unequal. This brings about a question of whether the CDW is a single one with bi-axis or two uniaxial CDWs in two orthorhombic domains.

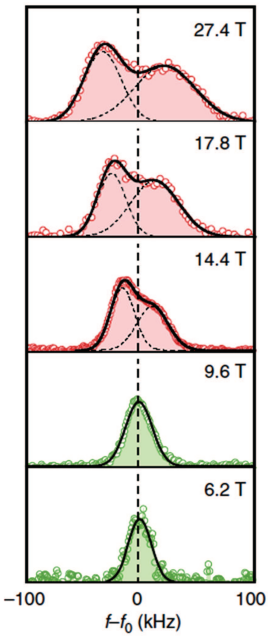


Fig. 12. The ^{17}O NMR evidence of charge order in $YBa_2Cu_3O_{6.56}$ (from Ref. [44]).

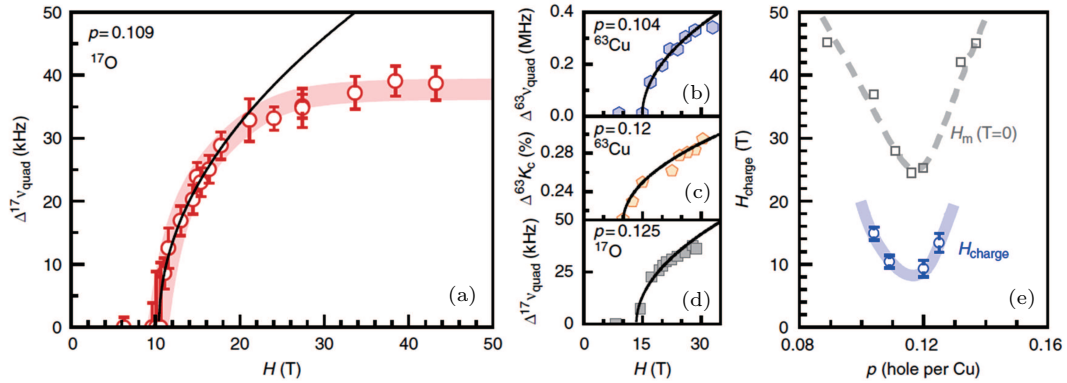


Fig. 13. Quantum phase transition to the charge-ordered state (from Ref. [44]).

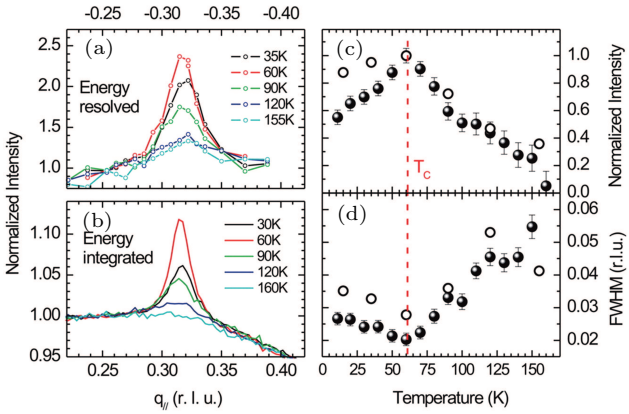


Fig. 14. Temperature dependence of the CDW signal obtained by resonant soft x-ray scattering in $YBa_2Cu_3O_{6.6}$ (from Ref. [45]).

Meanwhile, a similar result was obtained in another work with hard x-ray technique under external magnetic field up to 17 T. They found that the CDW under zero field can be enhanced by the magnetic field below the superconducting transition temperature.[46] The results of the hard x-ray experiment in three-dimensional reciprocal space are shown in Fig. 15. Two diffraction peaks due to CDW appear at the same in-plane wave vectors as the previous work. The rather wide lineshape in reciprocal space means a short-range modulation along c-axis with 0.6 lattice unit, which suggests a 2D nature for CDW. Above T_c, there is no any magnetic field effect on CDW signal while below T_c the CDW signal shows a remarkable en-

hancement with the application of the magnetic field. This is a direct evidence for the competition between CDW and superconductivity. Under the magnetic field of 17 T, the in-plane correlation length reaches ~ 95 Å (~ 25 lattice units) at 2 K, which is still a short-range CDW. Here, it should be noted that the onset temperature of CDW observed by x-ray technique is much higher than that determined by NMR technique. One plausible reason is different timescales. Usually, the timescale for x-ray technique is much shorter than that for NMR technique. Therefore, although a fluctuating CDW might be absent in a NMR timescale, it can be still observed by the x-ray technique. In contrast, another opinion on this issue is that there are two different CDW phases.[47] Next, we will discuss this possibility with more details.

Wu *et al.* carefully studied the low-field NMR spectra and found evidence for another short-range CDW different from the one under high magnetic field.[48] As shown in Fig. 17, the broadening effects of satellites and central line show a similar temperature-dependent behavior but with distinct magnitudes upon cooling below $T_{\rm onset} \approx 140$–$170$ K. From the previous section, we have learnt that the satellites are broadened by both electric quadrupole and magnetic contributions while the central line is only affected by the magnetic contribution. When a short-range CDW appears, although both the quadrupole broadening $\delta\nu_{\rm quad}$ and the magnetic broadening $\delta\nu_{\rm magn}$ should be taken into account for the linewidth, only the magnetic contribution appears on both the central line and the satellites with the same magnitude. In this case, the magnitude of the broadening effect for satellites and central line should be different, just as what we see in Fig. 17. Similar situation is also observed for NMR spectra splitting at the long-range CDW state under high magnetic field. It should be noted that in contrast to that the splitting only appearing at Cu2F sites,[37] the above broadening exists at both Cu2E and Cu2F sites, which also supports a 2D nature. Based on these results, the difference between x-ray and NMR results strongly suggests two distinct CDW phases in the H–T phase diagram. The field-induced 3D CDW phase under high magnetic field causes a remarkable splitting of NMR lines. The other 2D CDW phase under zero magnetic field is related to the significant quadrupole broadening of the NMR statellites. These two CDW phases have different charge modulation patterns. Therefore, it is quite clear that there are two different CDW phases in the H–T phase diagram. The following part will discuss the relationship between these two distinct CDW phases. In addition, since the broadenings of O sites along different Cu–O bonds show different values as shown in Figs. 17(a) and 17(b), the above NMR results due to a short-range CDW phase also suggest a possible intra-unit-cell nematic order, which is consistent with the proposal of biaxial CDW debated in previous x-ray work.[45]

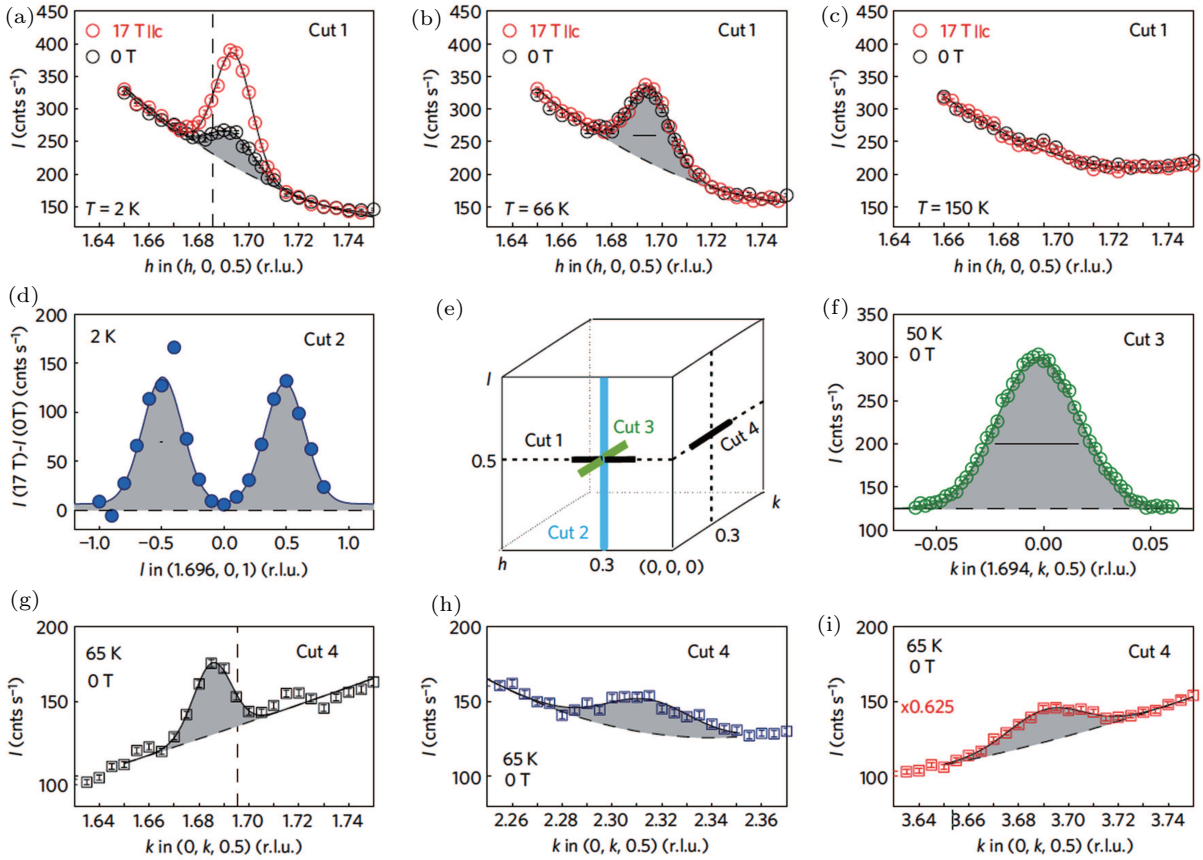


Fig. 15. Incommensurate charge-density-wave order (from Ref. [46]).

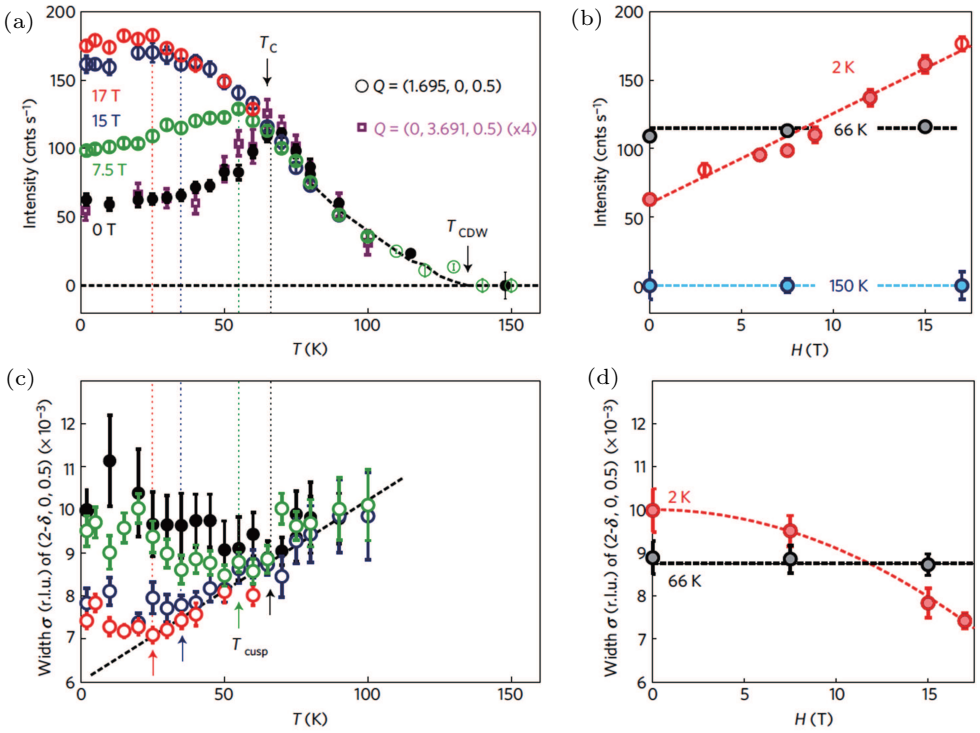


Fig. 16. Competition between charge-density-wave order and superconductivity (from Ref. [46]).

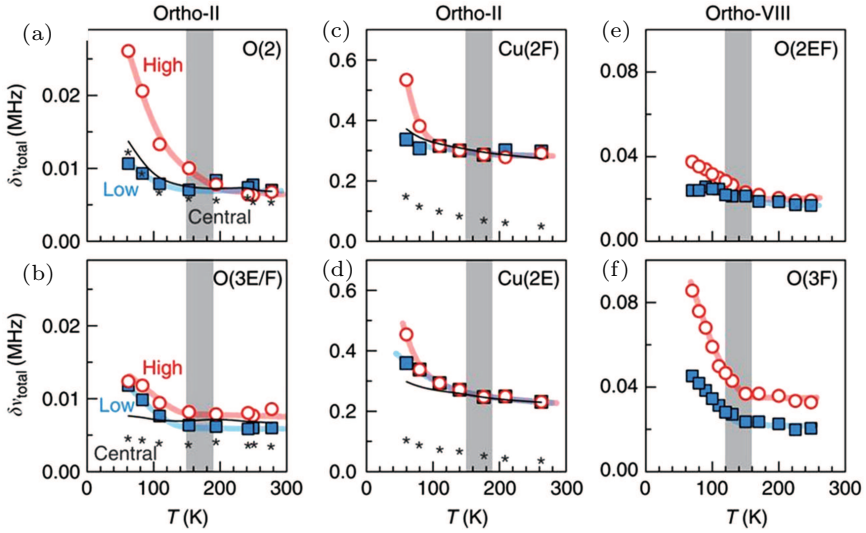


Fig. 17. Qualitative evidence of static charge modulation (from Ref. [48]).

Gerber *et al.* presented a pretty work with magnetic field up to 28 T by method of x-ray scattering at the x-ray free electron laser (FEL) whose high brilliance enabled detection of weak CDW signals.[49] The previous work was reproduced that the short-range correlated incommensurate 2D CDW order develops to maximum at T_c without external field. Thanks to the synchronization of millisecond pulsed magnetic field and femtosecond x-ray FEL pulses in their measurements, an intriguing low temperature 3D CDW order is revealed under high fields (> 15 T). The comparison of the temperature dependent evolution between these two CDW features is shown in Fig. 18. Instead of centering at $l \sim 0.5$, the new revealed 3D CDW locates in $l \sim 1$ in reciprocal space and is significantly enhanced with increasing magnetic field. As shown in Fig. 18(c), the temperature dependent intensity of this 3D CDW is consistent with the early high field NMR measurements, suggesting a same origination.[37] The two CDWs coexist at high field and have the same incommensurate in-plane components of the Q-vector (Fig. 19). While, the correlation length of the field induced one is over ~ 180 Å alone b-axis and ~ 50 Å (4–5 lattice units) alone c-axis at 28 T (Fig. 19). Such long correlation length indicates its 3D nature and rules out the possible origination of this CDW as a result of field aligned CDW regions associated with vortices.

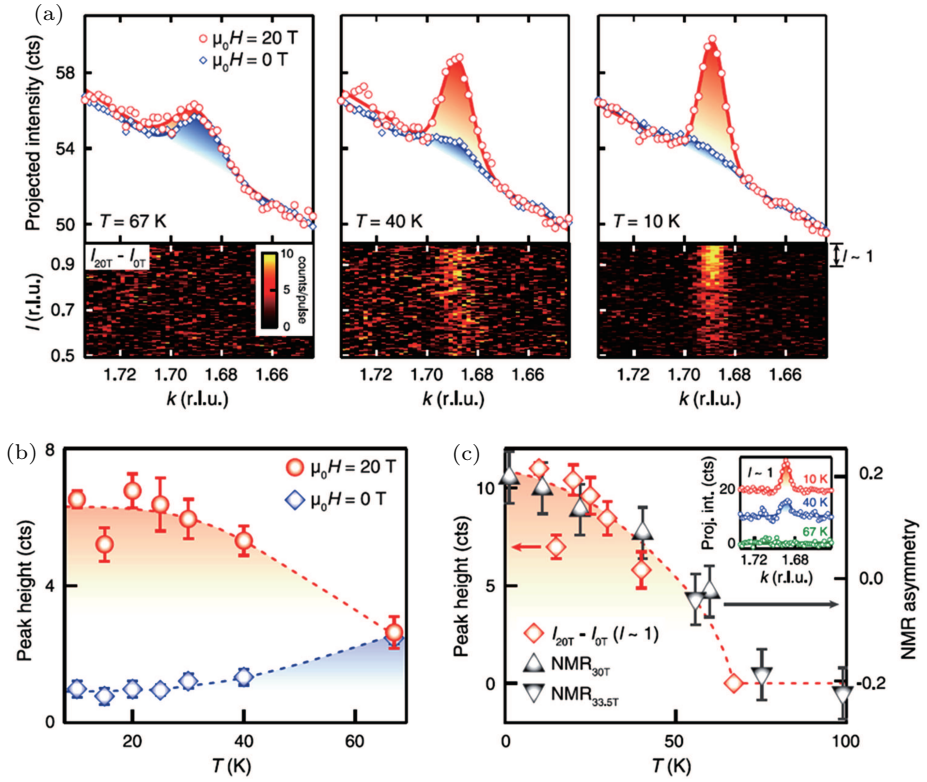


Fig. 18. Temperature dependence of the CDW order at $H = 0$, 20 T (from Ref. [49]).

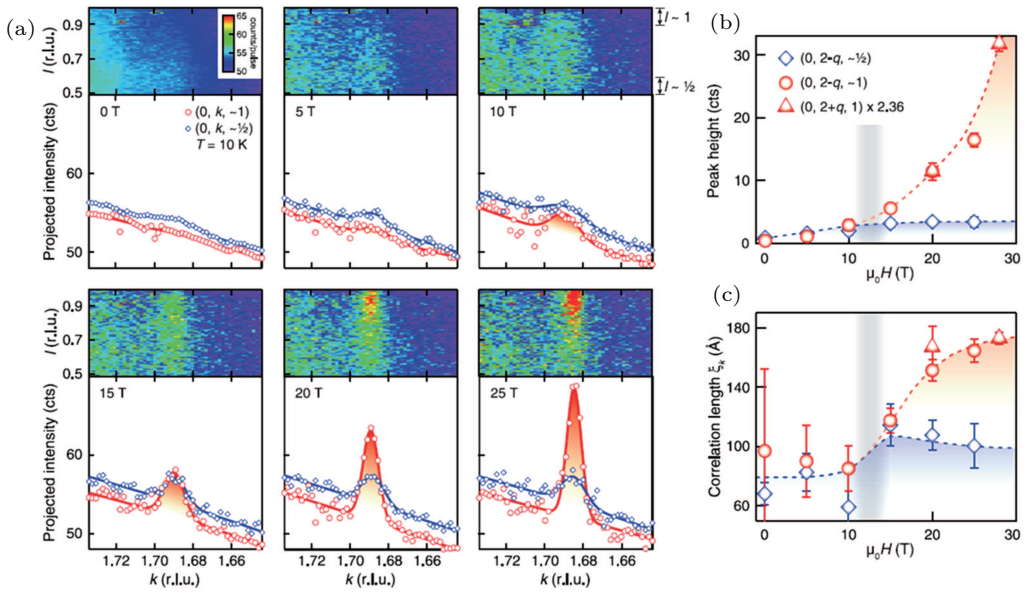


Fig. 19. Field dependence of the CDW order at $T = 10$ K (from Ref. [49]).

Chang *et al.* have carried out systematic high field hard x-ray scattering experiments on $YBa_2Cu_3O_{6+x}$ systems which put forward the study of the detail structure of the CDW order and explored the doping, field, and temperature dependent phase diagram of these systems.[50] As shown in Fig. 20, they confirmed the sudden appearance of an additional 3D CDW order at high fields in $YBa_2Cu_3O_{6.67}$ (hole doping ~ 0.123). They also found that the effects of applying magnetic fields are very different on the two in-plane components (q_a, q_b) of the CDW. With increasing magnetic field, the q_a correlation simply becomes stronger without any extra modulations. While for the q_b correlations, significant enhancement of the correlation length ξ_b is observed and accompanied with an $l\sim 1$ scattering peak emerged when the magnetic field is beyond 10 T. As shown in Fig. 21(a), the 3D CDW breaks the mirror symmetry of an individual CuO_2 bilayer which is the same as the lower field one, but the atomic displacements in adjacent bilayers are in phase. As sketched in Figs. 21(b)–21(d),

the field induced CDW can be weakly pinned by impurities in some regions of the sample to form fully 3D coherence and static with time scale > 0.1 ms as inferred from the NMR experiments.[37,48] The identified new field induced anisotropy in the CDW also answers the question mentioned above, that there are two in-plane uniaxial orthorhombic domains at high fields. All these suggest a field induced phase transition in YBCO, which implies that the magnetic field would enlarge the in-plane anisotropies of the CDW through enhancement of the correlations alone b-axis and in turn modify the coupling between the CuO_2 bilayers (Fig. 22(a)). Besides, from the doping–magnetic-field phase diagram (Fig. 22(b)), the 3D CDW order is most easily stabilized for doping around $p = 0.11$–0.12. Most recently, a quantum critical point (QCP) at $p = 0.08$ where the CDW can be formed with applying magnetic fields was revealed as shown in Fig. 23.[51]

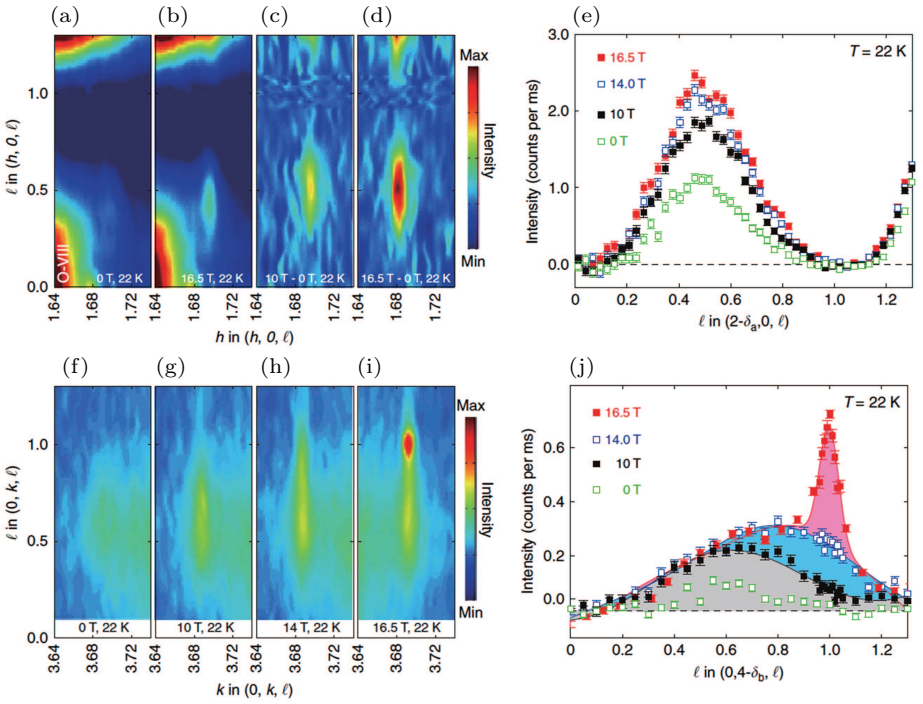


Fig. 20. Charge density wave correlations induced by a magnetic field in $YBa_2Cu_3O_{6.67}$ (from Ref. [50]).

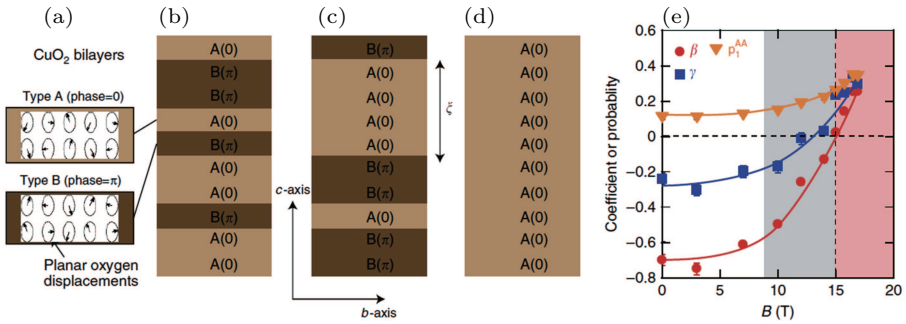


Fig. 21. Magnetic field effect on c-axis correlations in $YBa_2Cu_3O_{6.67}$ (from Ref. [50]).

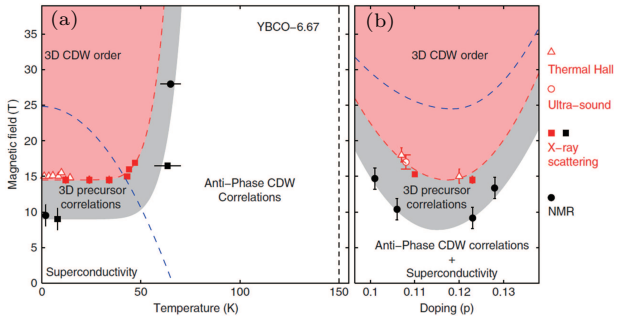


Fig. 22. Phase diagram of $YBa_2Cu_3O_{6+x}$ (from Ref. [50]).

At this stage, we shall draw a short summary about H–T phase diagram of YBCO.[52] As shown in Fig. 24, at high temperatures, only short-range 2D CDW correlation has been observed. Under low field region, the superconductivity overcomes the 2D CDW order at $T_c \sim 60$ K. As superconductivity is gradually suppressed by magnetic field, a sharp phase boundary emerges (~ 15 T) where a 3D CDW order sets in. Under higher fields, the 3D CDW takes place of the superconductivity as the new ground state of the system. Intriguingly, the two kinds of CDW cannot simply convert into one another. They coexist with each other in different domains under high fields and low temperatures. CDW has been known to occur

in many low-dimensional metals since last century. But how exactly the wave is triggered by cooperation between different degrees-of-freedom is still elusive and hot debated, especially in 2D systems. Cuprates are not only 2D metals, they are particularly complex ones with strongly correlated electrons and multi-order competing phase diagrams. To figure out the origin of the CDW is a hard theoretical task, much less its connection to superconductivity (though all experiments point to an evident competition between superconductivity and CDW order). Nevertheless, instructive insights from the experimental side are still expected. Some outstanding puzzles and effects are left to be explored, such as, what exactly is the role played by the inter-layer chain-oxygen defects? (only help to forming antiphase charge oscillations in two consecutive CuO_2 bilayers?). How about the pinning effects of the disorder? (stabilizing the 2D CDW fluctuating correlation into short-range order and help to establish fully 3D coherence of the 3D CDW order?). How the electronic structure and Fermi surface topology will evolve with CDW setting in? (reconstruction, new gap opening, and loss of density of states?). What will happen at even higher fields? (will two kinds of CDWs still coexist with each other or the 3D CDW finally overwhelms the 2D CDW even at high temperatures?). What is the relation between the CDW and the pseudogap? Can similar phenomena take place in other cuprate systems? With these thoughts in mind, next we will move on to the discussions of specific cases and gather some newest experimental progresses on part of these interesting issues.

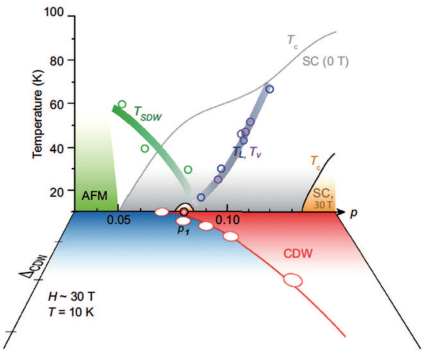


Fig. 23. A sketch of the YBCO phase diagram in the heavily underdoped regime with several other measurements superimposed (from Ref. [51]).

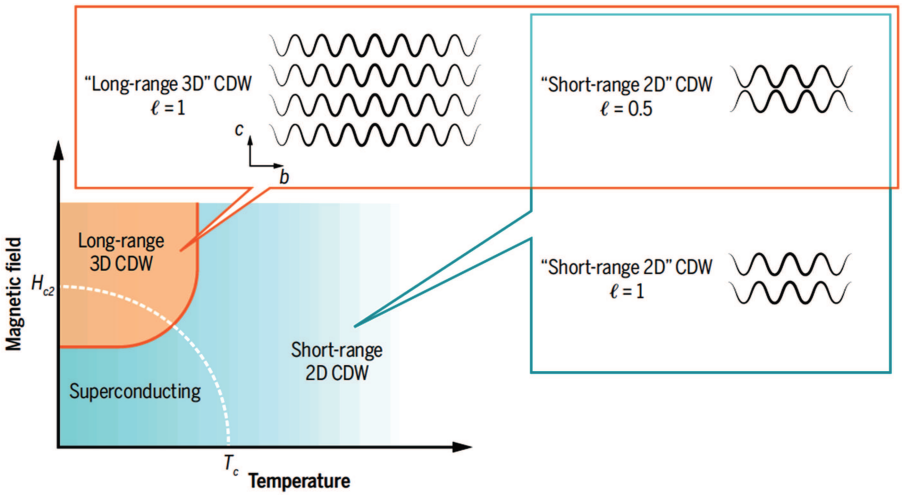


Fig. 24. The H–T phase diagram of YBCO (from Ref. [52]).

Recently, pieces of important information about the microscopic nature of the CDW have been revealed by Zhou *et al.*[53] Through meticulous analysis of the ^{17}O NMR spectra in several $YBa_2Cu_3O_y$ samples with different hole doping levels, they found an anomalous distribution of local density of states (DOS) on in-plane oxygen sites which results in asymmetric NMR spectra as shown in Fig. 25. By using bi-Gaussian fittings on the skewed peaks, they figured out that the asymmetry arises from the broadening of the right (high frequency) part of the line (ω_R in Figs. 26(a) and 26(b)). Meanwhile considering the continuous aspect of the line shapes, they inferred that $^{17}K_{spin}$ is maximal at relatively few locations and decays over a typical distance much larger than a lattice step. To some extent, such Knight shift distribution is rare. For instance, the system is far away from any magnetic order and the vortex lattice if any is negligible at such high fields. Besides, staggered magnetization produced by oxygen vacancies in the chains or impurities in the planes only leads to symmetric broadenings. In fact, the interference between CDW and Friedel oscillations would yield an asymmetric charge-density distribution. While if so, an accompanied prominent quadrupolar effect which influences differently on the satellite and central lines should be observed. On the other hand, locally promoted DOS at the Fermi level would provide an explanation to this result. But, unlike the case in the presence of Anderson localization, the locally enhanced DOS in YBCO systems most likely originated from the bounded (in-gap) electronic states. After ruling out various types of al-

ternative candidates such as the Andreev bound states, short-range fluctuating pairing-density-wave (PDW) states (none of these are static at NMR time scale), and the defect-induced bound states in the chains (inconsistent onset fields and missing in optimally-doped samples), the author finally ascribed the skewness of the peaks to the defect-induced bound states in the CuO_2 planes. Another remarkable character of this spatial distribution of local fields is that it seems arises only in conjunction with long-range CDW order as they share similar field and temperature dependent behavior which can be scaled with each other (Figs. 26(c) and 26(d)). As shown in Fig. 27, this kind of bound state widely exists in YBCO samples with different doping levels. Since the defects in the Cu–O chains constitute the main source of electronic scattering ubiquitously in oxygen-ordered YBCO, the bound states should be intimately related to it. While, from above analysis we know that the quasiparticle is not directly scattered by defects in the Cu–O chains, which leaves a paradox. Clarifying which aspect of the CDW is crucial in the formation of the bound states should be informative on its microscopic nature. An indication is that the c-axis coherence of the high filed 3D CDW order seems irrelevant to the formation of such bound states. Interestingly, the author pointed out that disorder induced bound states are widely observed among different sample systems (iron-based superconductors, heavy fermion systems, surface of topological insulators, etc) and they have been argued to be a generic property of metals with Dirac-type electronic dispersion.[54–58] The presence of a Dirac cone in the band structure would then provide clues on the reconstructed Fermi surface in high fields.[59]

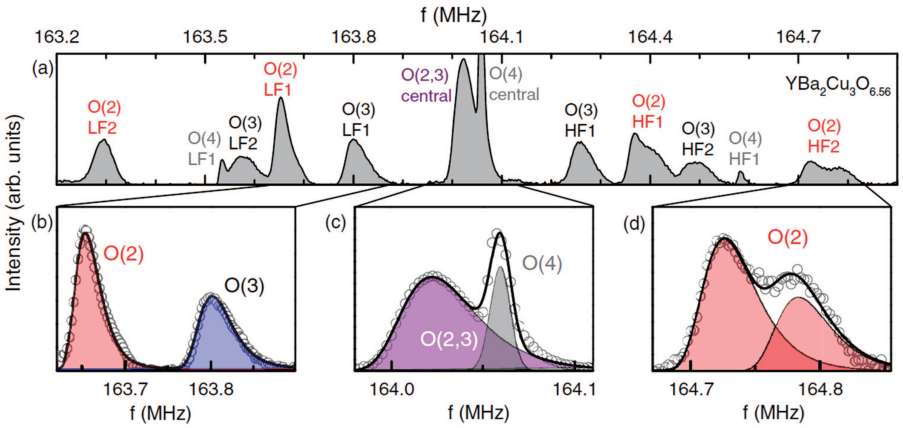


Fig. 25. The ^{17}O NMR spectrum of $YBa_2Cu_3O_{6.56}$ at $T = 3$ K and $H \simeq 28.5$ T (from Ref. [53]).

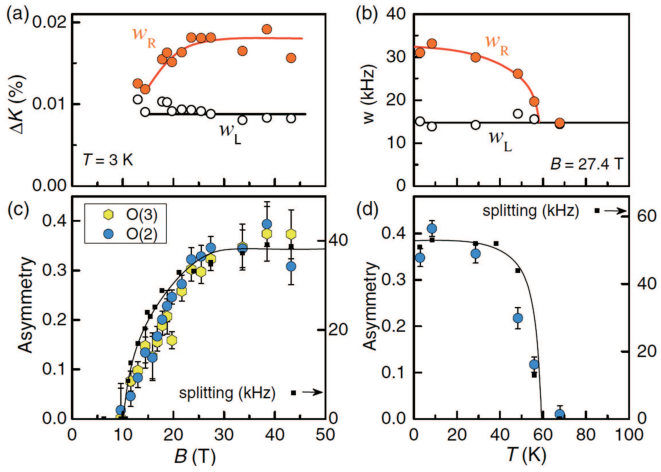


Fig. 26. Field and temperature dependence of ω_R, ω_L, and calculated asymmetry (from Ref. [53]).

Another excellent work done by Zhou *et al.* is the microscopic determination of the upper critical field H_{c2} of the YBCO systems.[60] Using the ^{17}O nuclei as a local probe, they can detect the field dependent intrinsic spin susceptibility χ_{spin} (mainly contributed from the $N(E_F)$ (DOS at the Fermi level) at low temperature) through measurements of the Knight shift at varied fields. As shown in Fig. 28, a clear saturation of K_{spin} is observed at high fields and the kinks signal the arrival of the upper critical filed for each sample. Plotting the determined H_{c2} data obtaining from different experimental methods on one graph shows a good consistence that H_{c2} in $YBa_2Cu_3O_y$ has a pronounced depression around $p = 0.11$–0.12 where it reaches values as low as ~ 20 T (Fig. 29). After subtraction of orbital shift K_{orb} and diamagnetic shift K_{dia}, a linearly field dependent K_{spin} seems more physically to fit their data below H_{c2}. Following their analysis will lead to identification of a sizable residual K_{spin}: K_0 ($K_0/K(H_{c2}) \sim 30\% \pm 1\%$) at zero field which is to say a residual $N(E_F)$. As shown in Fig. 30, the residual $N(E_F)$ is positively related to the concentration of disorder. While, extrapolating this relation to zero-width limit (free of disorder) still yields nonzero $N(E_F)$. This suggests an intrinsic $N(E_F)$ preserved in the superconducting state, which agrees with the results of specific heat measurement.[61] Note that, $K_{spin} \propto \sqrt{H/H_{c2}}$ is supposed to be the general case in cuprates at $T \ll T_c$ as expected for the Doppler shift of the quasiparticles outside the vortex cores in d-wave superconductors. So the linearity between H and K_{spin} is elusive which asks for further studies. One possible explanation they proposed is

that Zeeman energy of the nodal quasiparticles could exceed the Doppler energy when the high field induces changes in the Fermi surface. In their experiments, they did not see any sign of the existence of vortex solids at high fields (> 30 T), suggesting that vortex melting transition detected in other experiments may arises from some extrinsic effects, e.g., disorder induced heterogeneous regions with anomalously high H_{c2}. Intriguingly, they also estimated the relative magnitudes of the saturated K_{spin} at high fields and the K_{spin} at high temperature of a nearly optimally doped sample. The small DOS remaining in high fields ($\sim 18\%$) demonstrates that the non-superconducting ground state has a large pseudogap separating from the superconducting gap. In addition, they also found that K_{spin} does not undergo any significant change at either H_{CDW}^{2D} (10–20 T) or H_{CDW}^{3D} (5–10 T higher than H_{CDW}^{2D}). The absence of a decrease of K_{spin} at the CDW transition indicates that long-range CDW order does not produce substantial gapping of quasiparticle excitations. This means either that the Fermi surface reconstruction is totally unrelated to the CDW or that the short-range CDW modulations presenting at any field already deplete $N(E_F)$ before the transition toward long-range order.

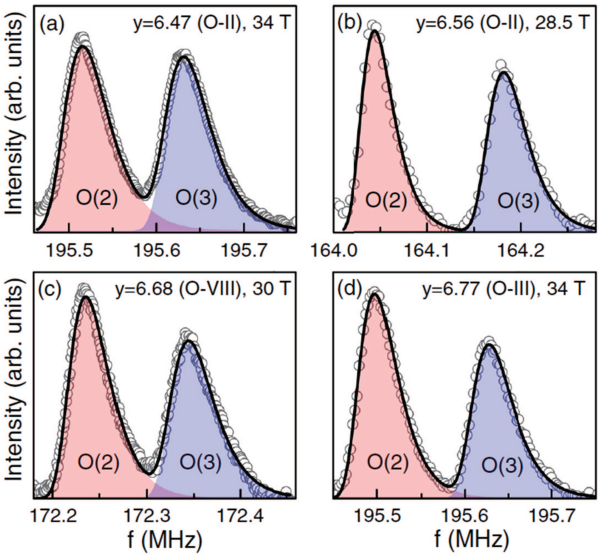


Fig. 27. O(2) and O(3) first low-frequency quadrupole satellites showing similar asymmetric profiles at $T \simeq 2$ K for four different samples (from Ref. [53]).

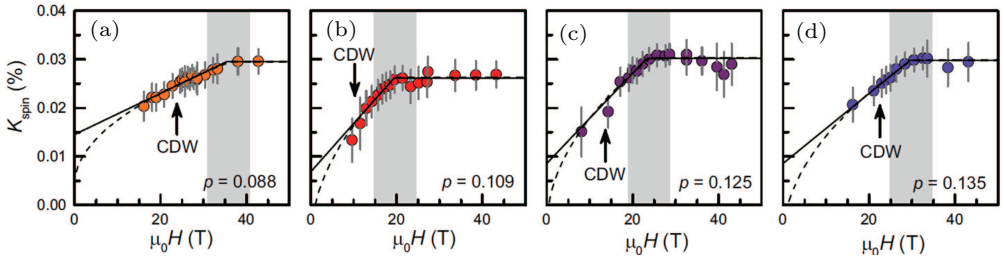


Fig. 28. Magnetic-field dependence of (the spin part of) ^{17}O(3) Knight shift in four different samples (from Ref. [60]).

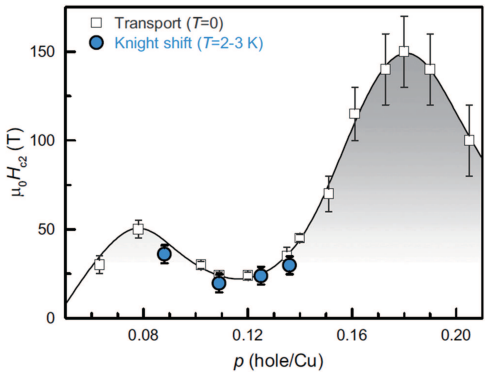


Fig. 29. Comparison of the determined H_{c2} data obtained from different experimental methods (from Ref. [60]).

To take a step on further understanding of the electronic structure at the Fermi level in YBCO systems at high fields, Kačmarčík *et al.* made comprehensive NMR and specific heat investigations on under-doped $YBa_2Cu_3O_y$ samples.[62] As expected, their experimental results confirm the existence of a saturated DOS above a characteristic field H_{DOS} at low temperatures (Fig. 31). Furthermore, an important feature about H_{DOS} is that its temperature dependence $H_{DOS}(T)$ displays a clear inflection when the field-induced long-range CDW order develops. As shown in Fig. 32, $H_{DOS}(T)$ first increases with temperature lowering, then after a subsequent plateau it sharply increases below ~ 10 K, tending towards H_{c2} for $T \to 0$, resulting in an S shape. At the same temperature range (< 10 K), an overshoot of specific heat ($T/T_c \sim 1/30$) is observed which is very unusual. As mentioned above, the vortex melting field is significantly lower than H_{DOS}, which indicates that the saturation of the DOS cannot be related to the melting of the vortex solid or an accidental compensation of the decrement from promoting CDW and increment from suppression of superconductivity. In principle, the constant DOS could be due to entering into a new type of gapless superconducting state, but the author failed to find any theoretical supports. It is also worth noting that the phase diagrams of Fig. 32(b) and 32(c) leave little doubt that the unusual S shape of $H_{DOS}(T)$ directly results from the influence of the

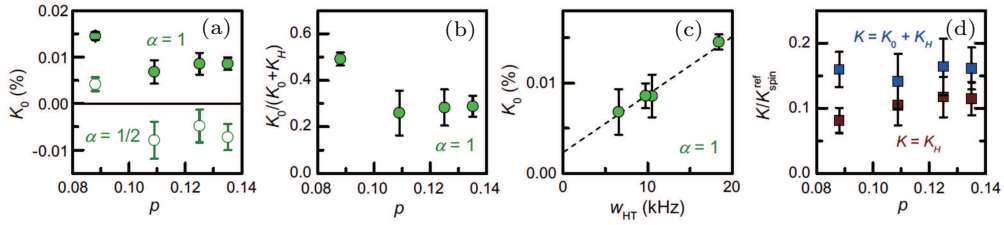


Fig. 30. Plotting the residual $K_{\rm spin}$ in the $H = 0$ limit (K_0) with varied parameters (from Ref. [60]).

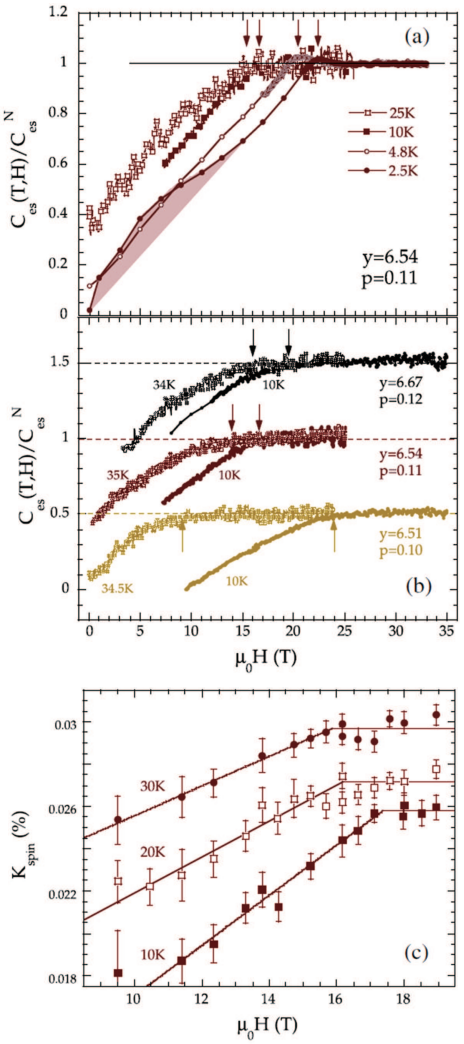


Fig. 31. Magnetic field dependence of the electronic specific heat, $C_{\rm es}(T,H)/T$, and $K_{\rm spin}$ (from Ref. [62]).

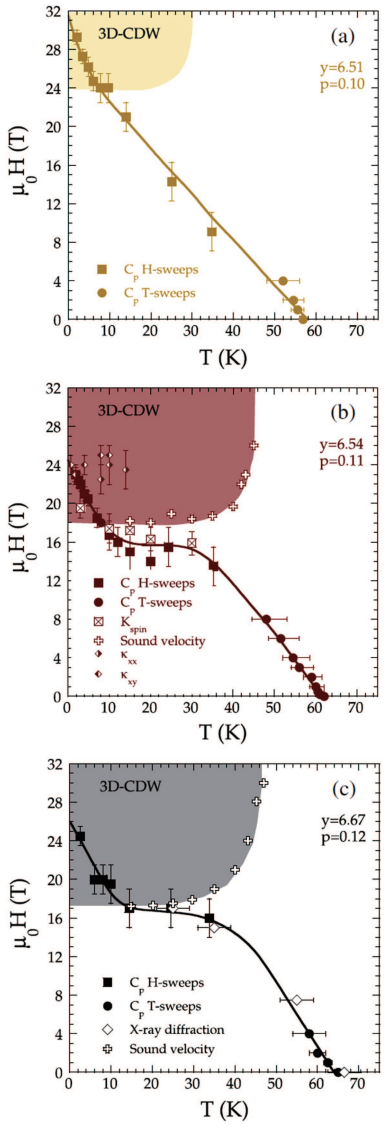


Fig. 32. The $H_{\rm DOS}$ versus temperature for the indicated doping contents (from Ref. [62]).

3D CDW order on superconductivity. The upswing of the $H_{\rm DOS}(T)$ line below ~ 10 K suggests that superconductivity eventually finds a way to accommodate the presence of the 3D long-range CDW order. One would image that, high magnetic fields may help to establish a PDW state in which spatial variations of the superconducting- and CDW-order parameters are intertwined.[63] Since it has been proposed that the 3D CDW is actually a consequence of a primary PDW order,[64] the author claimed that the above-proposed interpretation of their data seems to fit more naturally with the view that the PDW order is stabilized only in the coexistence region by the presence of an independent 3D CDW order.

4. High-field NMR study on charge stripe order in Bi2201 system

In the early days, dense studies on charge stripe order were focus on another high-$T_{\rm c}$ cuprates family — Bi-based cuprates.[21–23,47] In fact, real-space imagination of CO by STM were firstly realized on Bi-based cuprates.[21] Through applying an external magnetic field (5 T perpendicular to the CuO_2 plane), fourfold, bidirectional modulations of the local DOS can be clearly imaged in the vortex

cores (Fig. 33).[47] The observed CO is confirmed to be non-dispersive over an extended energy range and exists above 100 K which rules out the possible origination as a quasi-particle interference (QPI) pattern.[22,23] Latter STM experiments on Na doped $Ca_2CuO_2Cl_2$ (Na-CCOC) revealed similar features (nearly period-4) of the CO in Bi-based cuprates.[65] In recent years, the detail structure and doping dependent phase diagram of Bi2212 and Na-CCOC have been intensively studied.[66–68] Evidence for charge order in single-layered Bi-based compounds, $Bi_{2-y}Pb_ySr_{2-z}La_zCuO_{6+\delta}$ (Bi2201), was also reported.[69] Real and reciprocal space studies on the temperature evolution of CDW/CO in Bi2212 and Bi2201 systems have revealed possible connections between charge order and the pseudogap state.[11,70] The doping dependent CDW wave vector seems to intimate relate to the hot spots of the Fermi surface by comparison between RXS and ARPES results.[71,72] Previous Knight shift measurements also detect residual DOS in the pseudogap states at high fields and it shows a non-trivial carrier concentration dependence (an abrupt decrease when it is close to Mott transition which suggests a symmetry breaking without magnetic ordering).[73] The underlying physics of the normal states are still unclear. Special density modulations of the CDW/CO are predicted in the PDW scenario.[8,74]

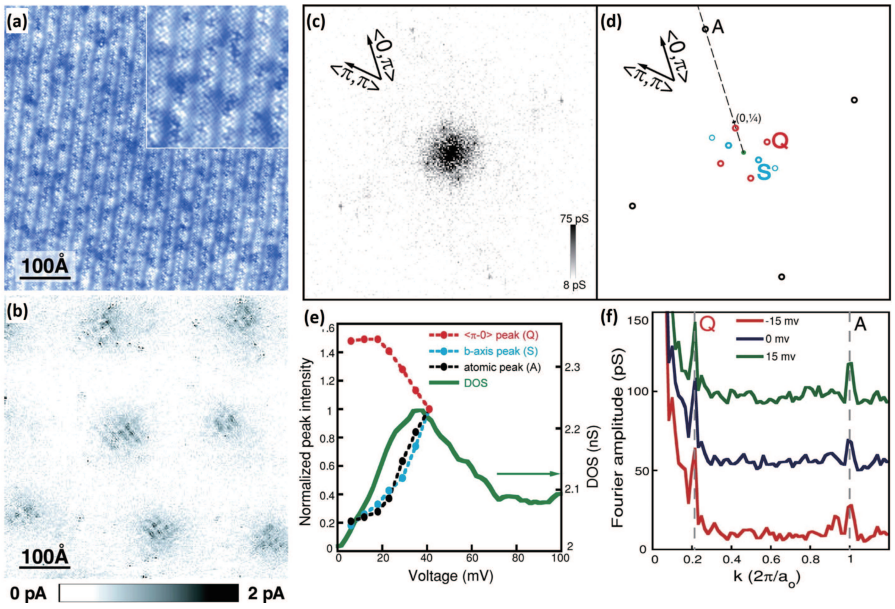


Fig. 33. STM explorations of charge order in Bi-based cuprates (from Refs. [21] and [23]).

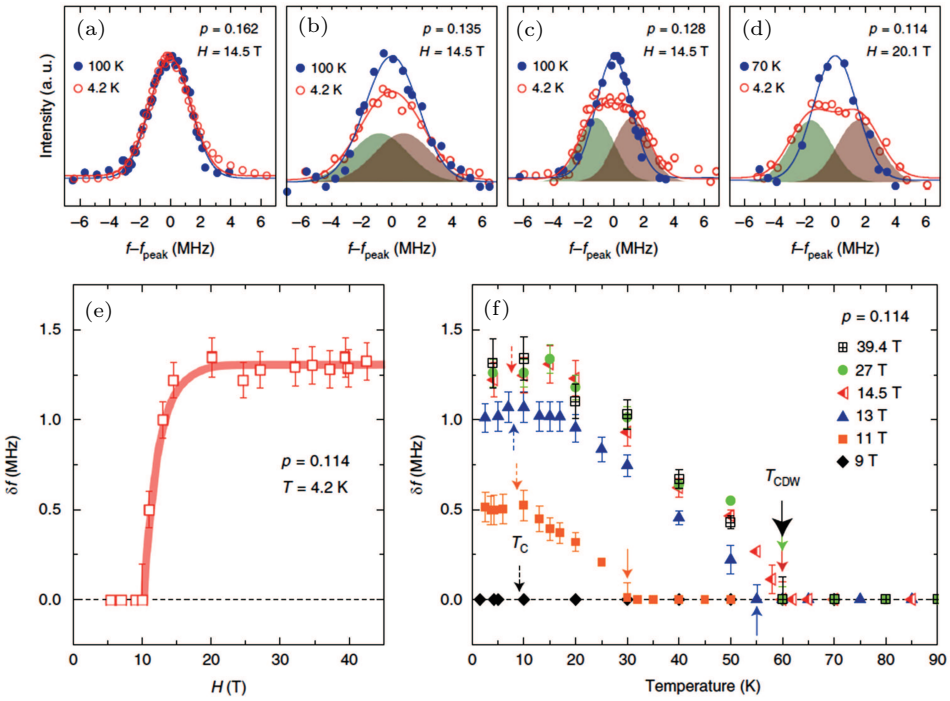


Fig. 34. Field and temperature evolution of NMR satellite line for under-doped Bi2201 (from Ref. [75]).

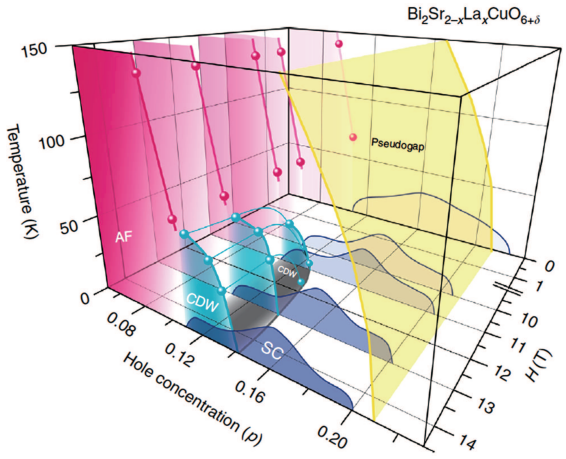


Fig. 35. Comprehensive phase diagrams of Bi2201 system with doping concentration, field, and temperature as tuning parameters (from Ref. [75]).

Besides, two major questions about the CDW in YBCO systems have been remained until now: one is that only out-of-plane field can induce the 3D CDW which leads to speculations that it is due to incipient CDW in the vortex cores that becomes overlapped as the field gets stronger, the other is the exact role played by the Cu–O chains. In order to get some insights on these questions, the high field investigations on CDW/CO in Bi2201 are highly needed. Kawasaki *et al.* made great experimental efforts on this subject. They have conducted NMR study on a couple of hole doped chainless systems — Bi2201 with in-plane magnetic fields up to 42.5 T.[75] As shown in Fig. 34, comparing with YBCO, similar NMR features have been observed in under-doped Bi2201 samples above a characteristic field $H_{\rm CDW}$ (~ 10 T), which demonstrate a field induced CDW (FICDW). The $H_{\rm CDW}$ is slightly lower than that in YBCO, suggesting that CDW has a similar energy scale across different class of cuprates. As shown in Fig. 35, with doping concentration, field, and temperature as tuning parameters, they obtained comprehensive phase diagrams of the Bi2201 system. There are several unique characters of the CDW in Bi2201 system. One remarkable point is that the onset temperature $T_{\rm CDW}$ takes over the antiferromagnetic order temperature $T_{\rm N}$ beyond a critical doping level at which superconductivity starts to emerge, and scales with the pseudogap temperature T^*. Since no vortex cores are created in CuO_2 planes under in-plane fields, the $H_{\rm CDW}$ and $T_{\rm CDW}$ of Bi2201 are more related with the doping concentration, which is different from the case in YBCO where $H_{\rm CDW}$ scales with H_{c2}. Considering the single CuO_2 layered structure without any Cu–O chains in Bi2201, the observed CDW is inherently 2D and a larger CDW amplitude (around twice of that of YBCO) is realized. Interestingly, in their experiments, the short-range CDW sets in right at T^* and the FICDW emerges far above the SC dome and finally coexists with it. Based on this, they proposed that the CDW in Bi2201 is closely related to the pseudogap (or to say the pseudogap is the incipient CDW in Bi2201).[76,77] At the moment, there still remain many elusive experimental results. But, without any doubt that the CDW order is another outstanding quantum phenomenon that should be addressed on the same footing as the AF spin order.

5. Possible charge ordering state in iron-based superconductors

Iron-based superconductors (IBS) are recognized as the second family of high-$T_{\rm c}$ superconductors.[78–82] Although the IBS exhibits a similar phase diagram as cuprates, the parent compounds of IBS are found to be multi-band correlated metals with striped AFM ground state[83] and the electronic correlation is strongly influenced by the Hund's coupling.[84] It would be very interesting to explore similar charge ordering phenomenon as cuprates in IBS, which would be important to build up a universal connection between high-$T_{\rm c}$ superconductivity and charge ordering.

Until now, although there are many efforts to explore charge ordering in IBS, the definitive evidence for charge ordering is still elusive. Initially, possible existence of CO states in slightly electron doped $LaOFeAs_{1-x}F_x$, $SmOFeAs_{1-x}F_x$ (1111 systems), and optimally hole doped $Ba_{1-x}K_xFe_2As_2$ (122 system) was claimed.[85–87] Lang *et al.* have conducted NQR study on series electron doped 1111 systems.[85] They proposed a nanoscale electronic order on the Fe sites stimulated by observing a clear two-peak structure in ^{75}As NQR spectra of slightly doped $LaOFeAs_{1-x}F_x$ and $SmOFeAs_{1-x}F_x$. Subsequently, Jasek *et al.* got similar conclusion through ^{57}Fe Mossbauer spectroscopy.[86,87] In recent years, more evidences for possible CO state have also been accumulated in heavily hole doped IBS — AFe_2As_2 (A = K, Rb, Cs) systems.[88–90] Wang *et al.* found an NMR line splitting with in-plane external field in pressurized KFe_2As_2 with $P =$ 2.42 GPa, suggesting a pressure induced checkboard-type CO.[88] Civardi *et al.* also found a possible CO state in $RbFe_2As_2$ under ambient pressure. Interestingly, in contrast to pressurized KFe_2As_2 and $RbFe_2As_2$, Li *et al.* found an NMR evidence for local B_{2g} nematic order in $CsFe_2As_2$,[90] which might be also related to possible CO state. However, all these phenomena in AF_2As_2 family are very sensitive on sample quality and further careful study is needed.[91] Lately, high-resolution ARPES study on hole doped 122 system (Na doped $BaFe_2As_2$) revealed a possible emergent charge order in the C_4 re-entrant phase.[92] The band splitting at the X point only in the C_4 re-entrant phase suggests a checkerboard CO which is compatible and strong coupled with the double-Q magnetic order (DQMO) in the C_4 re-entrant phase. The results are reminiscent of the intertwined electronic stripe order appearing at 1/8 doping in the $La_{2-x}Ba_xCuO_4$ cuprate system where the CO strongly couples to the spin order. In a short summary, although there are many intriguing phenomena relevant to the

possible CO state in IBS, whether these phenomena are intrinsic or universal for IBS is still elusive. Further experiments are urgently needed to figure out the above issue in near future.

6. Perspective

In this short review, we have introduced the recent high-field NMR progress on charge order in YBCO. Based on high-field NMR results, a field-induced charge order is discovered which is actually different from the following short-range charge order discovered by low-field x-ray scattering experiment. The implications of NMR results go beyond the microscopic explanation of quantum oscillation experiments. In correlated electrons system, quantum melting of electronic crystalline phase often gives rise to many novel electronic phases. In cuprate superconductors, melting the Mott insulating phase with carrier doping is believed to lead a quantum version of liquid crystal phase, the electronic nematicity, which breaks the rotational symmetry and exhibits a tight twist with high-T_c superconductivity. These NMR findings would be an important experimental evidence to support such physical scenario for high-T_c superconductivity. On the other hand, it would be an interesting work to search similar charge order in high-T_c Fe-based superconductors, which would be very important to unify both high-T_c families.

References

[1] Lee P A, Nagaosa N and Wen X G 2006 *Rev. Mod. Phys.* **78** 17
[2] Varma C M 1997 *Phys. Rev. B* **55** 14554
[3] Emery V J, Kivelson S A and Tranquada J M 1999 *Proc. Natl. Acad. Sci.* **96** 8814
[4] Kivelson S A, Aeppli G and Emery V J 2001 *Proc. Natl. Acad. Sci.* **98** 11903
[5] Zaanen J 2000 *Nature* **404** 714
[6] Sachdev S 2000 *Science* **288** 475
[7] Chakravarty S, Laughlin R B, Morr D K and Nayak C 2001 *Phys. Rev. B* **63** 094503
[8] Keimer B, Kivelson S A, Norman M R, Uchida S and Zaanen J 2015 *Nature* **518** 179
[9] Ando Y, Segawa K, Komiya S and Lavrov A N 2002 *Phys. Rev. Lett.* **88** 137005
[10] Lawler M J, Fujita K, Lee J, Schmidt A R, Kohsaka Y, Kim C K, Eisaki H, Uchida S, Davis J C, Sethna J P and Kim E A 2010 *Nature* **466** 347
[11] Parker C V, Aynajian P, da Silva Neto E H, Pushp A, Ono S, Wen J, Xu Z, Gu G and Yazdani A 2010 *Nature* **468** 677
[12] Hinkov V, Haug D, Fauque B, Bourges P, Sidis Y, Ivanov A, Bernhard C, Lin C T and Keimer B 2008 *Science* **319** 597
[13] Daou R, Chang J, LeBoeuf D, Olivier C C, Laliberte F, Leyraud N D, Ramshaw B J, Liang R X, Bonn D A, Hardy W N and Taillefer L 2010 *Nature* **463** 519
[14] LeBoeuf D, Doiron-Leyraud N, Levallois J, Daou R, Bonnemaison J B, Hussey N E, Balicas L, Ramshaw B J, Liang R, Bonn D A, Hardy W N, Adachi S, Proust C and Taillefer L 2007 *Nature* **450** 533
[15] LeBoeuf D, Doiron-Leyraud N, Vignolle B, Sutherl, M, Ramshaw B J, Levallois J, Daou R, Laliberté F, Cyr-Choinière O, Chang J, Jo Y J, Balicas L, Liang R, Bonn D A, Hardy W N, Proust C and Taillefer L 2011 *Phys. Rev. B* **83** 054506
[16] Laliberté F, Chang J, Doiron-Leyraud N, Hassinger E, Daou R, Rondeau M, Ramshaw B J, Liang R, Bonn D A, Hardy W N, Pyon S, Takayama T, Takagi H, Sheikin I, Malone L, Proust C, Behnia K and Taillefer L 2011 *Nat. Commun.* **2** 432
[17] Kivelson S A, Bindloss I P, Fradkin E, Oganesyan V, Tranquada J M, Kapitulnik A and Howald C 2003 *Rev. Mod. Phys.* **75** 1201
[18] Vojta M 2009 *Adv. Phys.* **58** 699
[19] Kivelson S A, Fradkin E and Emery V J 1998 *Nature* **393** 550
[20] Tranquada J M, Sternlieb B J, Axe J D, Nakamura Y and Uchida S 1995 *Nature* **375** 561
[21] Hoffman J E, Hudson E W, Lang K M, Madhavan V, Eisaki H, Uchida S and Davis J C 2002 *Science* **295** 466
[22] Howald C, Eisaki H, Kaneko N and Kapitulnik A 2003 *Proc. Natl. Acad. Sci.* **100** 9705
[23] Vershinin M 2004 *Science* **303** 1995
[24] Moler K 2010 *Nature* **468** 643
[25] Fujita M, Goka H, Yamada K, Tranquada J M and Regnault L P 2004 *Phys. Rev. B* **70** 104517
[26] Hücker M, v. Zimmermann M, Gu G D, Xu Z J, Wen J S, Xu G, Kang H J, Zheludev A and Tranquada J M 2011 *Phys. Rev. B* **83** 104506
[27] Abbamonte P, Rusydi A, Smadici S, Gu G D, Sawatzky G A and Feng D L 2005 *Nat. Phys.* **1** 155
[28] Fink J, Soltwisch V, Geck J, Schierle E, Weschke E and Büchner B 2011 *Phys. Rev. B* **83** 092503
[29] Wilkins S B, Dean M P M, Fink J, Hücker M, Geck J, Soltwisch V, Schierle E, Weschke E, Gu G, Uchida S, Ichikawa N, Tranquada J M and Hill J P 2011 *Phys. Rev. B* **84** 195101
[30] Hunt A W, Singer P M, Cederström A F and Imai T 2001 *Phys. Rev. B* **64** 134525
[31] Julien M H, Campana A, Rigamonti A, Carretta P, Borsa F, Kuhns P, Reyes A P, Moulton W G, Horvatić M, Berthier C, Vietkin A and Revcolevschi A 2001 *Phys. Rev. B* **63** 144508
[32] Curro N J, Hammel P C, Suh B J, Hücker M, Büchner B, Ammerahl U and Revcolevschi A 2000 *Phys. Rev. Lett.* **85** 642
[33] Grafe H J, Curro N J, Hücker M and Büchner B 2006 *Phys. Rev. Lett.* **96** 017002
[34] Doiron-Leyraud N, Proust C, LeBoeuf D, Levallois J, Bonnemaison J B, Liang R, Bonn D A, Hardy W N and Taillefer L 2007 *Nature* **447** 565
[35] Sebastian S E, Harrison N and Lonzarich G G 2011 *Philos. Trans. R. Soc. Math. Phys. Eng. Sci.* **369** 1687
[36] Ramshaw B J, Vignolle B, Day J, Liang R, Hardy W N, Proust C and Bonn D A 2011 *Nat. Phys.* **7** 234
[37] Wu T, Mayaffre H, Krämer S, Horvatić M, Berthier C, Hardy W N, Liang R, Bonn D A and Julien M H 2011 *Nature* **477** 191
[38] Hammerath F 2012 *Magnetism and Superconductivity in Iron-based Superconductors as Probed by Nuclear Magnetic Resonance* (Fachmedien Wiesbaden: Springer) p. 3
[39] Ghoshray K, Pahari B, Ghoshray A, Eremenko V V, Sirenko V A and Suits B H 2009 *J. Phys. Condens. Matter* **21** 155701
[40] Freude E D and Haase J 1993 *Quadrupole Effects in Solid-state Nuclear Magnetic Resonance Special Applications* (Berlin Heidelberg: Springer Science & Business Media) p. 1
[41] Blinc R and Apih T 2002 *Prog. Nucl. Magn. Reson. Spectrosc.* **41** 49
[42] Butz T 2013 *Nuclear Spectroscopy on Charge Density Wave Systems* (The Netherlands: Kluwer Academic Publishers) p. 113
[43] Yamani Z, MacFarlane W A, Statt B W, Bonn D, Liang R and Hardy W N 2004 *Phys. C Supercond.* **405** 227
[44] Wu T, Mayaffre H, Krämer S, Horvatić M, Berthier C, Kuhns P L, Reyes A P, Liang R, Hardy W N, Bonn D A and Julien M H 2013 *Nat. Commun.* **4** 2113
[45] Ghiringhelli G, Tacon M L, Minola M, Blanco-Canosa S, Mazzoli C, Brookes N B, De Luca G M, Frano A, Hawthorn D G, He F, Loew T, Sala M M, Peets D C, Salluzzo M, Schierle E, Sutarto R, Sawatzky G A, Weschke E, Keimer B and Braicovich L 2012 *Science* **337** 821
[46] Chang J, Blackburn E, Holmes A T, Christensen N B, Larsen J, Mesot J, Liang R, Bonn D A, Hardy W N, Watenphul A, v. M, Forgan E M and Hayden S M 2012 *Nat. Phys.* **8** 871
[47] Comin R and Damascelli A 2016 *Annu. Rev. Matter Phys.* **7** 369
[48] Wu T, Mayaffre H, Krämer S, Horvatić M, Berthier C, Hardy W N, Liang R, Bonn D A and Julien M H 2015 *Nat. Commun.* **6** 6438
[49] Gerber S, Jang H, Nojiri H, Matsuzawa S, Yasumura H, Bonn D A, Liang R, Hardy W N, Islam Z, Mehta A, Song S, Sikorski M, Stefanescu D, Feng Y, Kivelson S A, Devereaux T P, Shen Z X, Kao C C, Lee W S, Zhu D and Lee J S 2015 *Science* **350** 949
[50] Chang J, Blackburn E, Ivashko O, Holmes A T, Christensen N B, Hücker M, Liang R, Bonn D A, Hardy W N, Rütt U, v. M, Forgan E M and Hayden S M 2016 *Nat. Commun.* **7** 11494

[51] Jang H, Lee W S, Song S, Nojiri H, Matsuzawa S, Yasumura H, Huang H, Liu Y J, Porras J, Minola M, Keimer B, Hastings J, Zhu D, Devereaux T P, Shen Z X, Kao C C and Lee J S 2018 *Phys. Rev. B* **97** 224513

[52] Julien M H 2015 *Science* **350** 914

[53] Zhou R, Hirata M, Wu T, Vinograd I, Mayaffre H, Krämer S, Horvatić M, Berthier C, Reyes A P, Kuhns P L, Liang R, Hardy W N, Bonn D A and Julien M H 2017 *Phys. Rev. Lett.* **118** 017001

[54] Yang H, Wang Z, Fang D, Deng Q, Wang Q H, Xiang Y Y, Yang Y and Wen H H 2013 *Nat. Commun.* **4** 2749

[55] Yin J X, Wu Z, Wang J H, Ye Z Y, Gong J, Hou X Y, Shan L, Li A, Liang X J, Wu X X, Li J, Ting C S, Wang Z Q, Hu J P, Hor P H, Ding H and Pan S H 2015 *Nat. Phys.* **11** 543

[56] Zhou B B, Misra S, da Silva Neto E H, Aynajian P, Baumbach R E, Thompson J D, Bauer E D and Yazdani A 2013 *Nat. Phys.* **9** 474

[57] Ugeda M M, Brihuega I, Guinea F and Gómez-Rodríguez J M 2010 *Phys. Rev. Lett.* **104** 096804

[58] Alpichshev Z, Biswas R R, Balatsky A V, Analytis J G, Chu J H, Fisher I R and Kapitulnik A 2012 *Phys. Rev. Lett.* **108** 206402

[59] Eberlein A, Metzner W, Sachdev S and Yamase H 2016 *Phys. Rev. Lett.* **117** 187001

[60] Zhou R, Hirata M, Wu T, Vinograd I, Mayaffre H, Krämer S, Reyes A P, Kuhns P L, Liang R, Hardy W N, Bonn D A and Julien M H 2017 *Proc. Natl. Acad. Sci. USA* **114** 13148

[61] Marcenat C, Demuer A, Beauvois K, Michon B, Grockowiak A, Liang R, Hardy W, Bonn D A and Klein T 2015 *Nat. Commun.* **6** 7927

[62] Kačmarčík J, Vinograd I, Michon B, Rydh A, Demuer A, Zhou R, Mayaffre H, Liang R, Hardy W N, Bonn D A, Doiron-Leyraud N, Taillefer L, Julien M H, Marcenat C and Klein T 2018 *Phys. Rev. Lett.* **121** 167002

[63] Fradkin E, Kivelson S A and Tranquada J M 2015 *Rev. Mod. Phys.* **87** 457

[64] Dai Z, Zhang Y H, Senthil T and Lee P A 2018 *Phys. Rev. B* **97** 174511

[65] Hanaguri T, Lupien C, Kohsaka Y, Lee D H, Azuma M, Takano M, Takagi H and Davis J C 2004 *Nature* **430** 1001

[66] Kohsaka Y, Taylor C, Fujita K, Schmidt A, Lupien C, Hanaguri T, Azuma M, Takano M, Eisaki H, Takagi H, Uchida S and Davis J C 2007 *Science* **315** 1380

[67] Kohsaka Y, Taylor C, Wahl P, Schmidt A, Lee J, Fujita K, Alldredge J W, McElroy K, Lee J, Eisaki H and Uchida S 2008 *Nature* **454** 1072

[68] Lee J, Fujita K, Schmidt A R, Kim C K, Eisaki H, Uchida S and Davis J C 2009 *Science* **325** 1099

[69] Wise W D, Boyer M C, Chatterjee K, Kondo T, Takeuchi T, Ikuta H, Wang Y and Hudson E W 2008 *Nat. Phys.* **4** 696

[70] da Silva Neto E H, Parker C V, Aynajian P, Pushp A, Yazdani A, Wen J, Xu Z and Gu G 2012 *Phys. Rev. B* **85** 104521

[71] Comin R, Frano A, Yee M M, Yoshida Y, Eisaki H, Schierle E, Weschke E, Sutarto R, He F, Soumyanarayanan A, He Yang, Le M, Elfimov I S, Hoffman Jennifer E, Sawatzky G A, Keimer B and Damascelli A 2014 *Science* **343** 360

[72] Peng Y, Salluzzo M, Sun X, Ponti A, Betto D, Ferretti A M, Fumagalli Kummer F K, Le Tacon M, Zhou X J, B N, Brookes, Braicovich L and Ghiringhelli G 2016 *Phys. Rev. B* **94** 184511

[73] Kawasaki S, Lin C, Kuhns P L, Reyes A P and Zheng G-q 2010 *Phys. Rev. Lett.* **105** 137002

[74] Lee P A 2014 *Phys. Rev. X* **4** 031017

[75] Kawasaki S, Li Z, Kitahashi M, Lin C T, Kuhns P L, Reyes A P and Zheng G 2017 *Nat. Commun.* **8** 1267

[76] Zhao L, Belvin C A, Liang R, Bonn D A, Hardy W N, Armitage N P and Hsieh D 2017 *Nat. Phys.* **13** 250

[77] He R H, Hashimoto M, Karapetyan H, Koralek J D, Hinton J P, Testaud J P, Nathan V, Yoshida Y, Yao H, Tanaka K, Meevasana W, Moore R G, Lu D H, Mo S K, Ishikado M, Eisaki H, Hussain Z, Devereaux T P, Kivelson S A, Orenstein J, Kapitulnik A and Shen Z X 2011 *Science* **331** 1579

[78] Takahashi H, Igawa K, Arii K, Kamihara Y, Hirano M and Hosono H 2008 *Nature* **453** 376

[79] Chen X H, Wu T, Wu G, Liu R H, Chen H and Fang D F 2008 *Nature* **453** 761

[80] Chen G F, Li Z, Wu D, Li G, Hu W Z, Dong J, Zheng P, Luo J L and Wang N L 2008 *Phys. Rev. Lett.* **100** 247002

[81] Ren Z A, Lu W, Yang J, Yi W, Shen X L, Li Z C, Che G C, Dong X L, Sun L L, Zhou F and Zhao Z X 2008 *Chin. Phys. Lett.* **25** 2215

[82] Ren Z A, Yang J, Lu W, Yi W, Che G C, Dong X L, Sun L L and Zhao Z X 2008 *Mater. Res. Innovat.* **12** 105

[83] Dai P, Hu J and Dagotto E 2012 *Nat. Phys.* **8** 709

[84] Haule K and Kotliar G 2009 *New J. Phys.* **11** 025021

[85] Lang G, Grafe H J, Paar D, Hammerath F, Manthey K, Behr G, Werner J and Büchner B 2010 *Phys. Rev. Lett.* **104** 097001

[86] Jasek A K, Komedera K, Błachowski A, Ruebenbauer K, Bukowski Z, Storey J G and Karpinski J 2014 *J. Alloys Compd.* **609** 150

[87] Jasek A K, Komedera K, Błachowski A, Ruebenbauer K, Lochmajer H, Zhigadlo N D and Rogacki K 2016 *J. Alloys Compd.* **658** 520

[88] Wang P S, Zhou P, Dai J, Zhang J, Ding X X, Lin H, Wen H H, Norm, B, Yu R and Yu W 2016 *Phys. Rev. B* **93** 085129

[89] Civardi E, Moroni M, Babij M, Bukowski Z and Carretta P 2016 *Phy. Rev. Lett.* **117** 217001

[90] Li J, Zhao D, Wu Y P, Li S J, Song D W, Zheng L X, Wang N Z, Luo X G, Sun Z, Wu T, Chen X H, Wu T and Chen X H 2016 arXiv:161104694[Cond-Mat]

[91] Moroni M, Prando G, Aswartham S, Morozov I, Bukowski Z, Büchner B, Grafe H J and Carretta P 2019 *Phys. Rev. B* **99** 235147

[92] Yi M, Frano A and Lu D H et al 2018 *Phys. Rev. Lett.* **121** 127001